2008-01-01

Experiment of All Solid-State Electrochemical Sensor for Surface Chemistry Analysis for Adhesive Bonding

Yao Ge
University of Miami, y.ge@umiami.edu

UNIVERSITY OF MIAMI

EXPERIMENT STUDY OF ALL SOLID-STATE ELECTROCHEMICAL SENSOR FOR SURFACE CHEMISTRY ANALYSIS FOR ADHESIVE BONDING

By

Yao Ge

A THESIS

Submitted to the Faculty
of the University of Miami
in partial fulfillment of the requirements for
the degree of Master of Science

Coral Gables, Florida

August 2008

UNIVERSITY OF MIAMI

A thesis submitted in partial fulfillment of
the requirements for the degree of
Master of Science

EXPERIMENT STUDY OF ALL SOLID-STATE ELECTROCHEMICAL SENSOR FOR SURFACE CHEMISTRY ANALYSIS FOR ADHESIVE BONDING

Yao Ge

Approved:

_____ Dr. Xiangyang Zhou Assistant Professor of Mechanical and Aerospace Engineering	_____ Dr. Terri A. Scandura Dean of the Graduate School
_____ Dr. Sohyung Cho Assistant Professor of Industrial Engineering	_____ Dr. Singiresu S.Rao Professor and Chair of Mechanical and Aerospace Engineering

_____
Dr. Weihua Zhang
Research Scientist of Applied Research Center
Florida International University

GE, YAO (M.S., Mechanical and Aerospace Engineering)
Experiment of All Solid-State Electrochemical Sensor for Surface Chemistry Analysis for Adhesive Bonding
(August 2008)

Abstract of a thesis at the University of Miami.

Thesis supervised by Professor Xiangyang Zhou.
No. of pages in text. (66)

This thesis presents: 1) literature review on adhesive bonding technologies in aviation industry including surface pretreatments (pre-preparation), surface quality assurance, and surface chemistry analysis methods; and 2) development and study of a novel solid-state electrochemical sensor for surface chemistry analysis of composite surfaces.

The performance of an adhesive bonding is greatly determined by the adherend's surface pretreatments which could increase surface tension, surface roughness, and change surface chemistry thereby increasing bond strength and durability of polymer composite adhesive joints. The primary goal of the surface pretreatments is to increase the surface roughness, surface energy, chemical activity, and cleanliness of the composite adherend as much as possible. Methods of surface pretreatments are reviewed in this paper, including: (1) abrasion/solvent cleaning; (2) grit blasting; (3) peel-ply; (4) tear-ply; (5) acid etching/anodizing; (6) corona discharge treatment; (7) plasma treatment; (8) flame treatment; (9) laser treatment; (10) others.

One of the critical issues in aviation industry for an adhesive bonding is to analyze the prepared composite surfaces using a nondestructive inspection (NDI) or nondestructive test (NDT) method to determine whether the quality of surfaces are

ready for the following bonding processes. Existing NDI methods include: (1) Near-Infrared; (2) Electrical potential; (3) Transient thermal NDT; (4) Electrical Impedance Spectroscopy (EIS); (5) Neutron radiography; and (6) X-ray Photoelectron Spectroscopy (XPS). However, up till now, these methods cannot provide definitive analysis or online and in-field analysis. Because of the non-availability of an on-line, in-field NDI method for surface chemistry analysis, excess or inadequate surface treatment and quality control processes may exist in the current aircraft manufacture processes incurring either a high cost or potentially weak adhesive bonds.

Electrochemical reactions usually occur in liquid electrolyte or on conducting electrode but not on non-conducting composite. Conventional electrochemical sensors involve liquid electrolytes which will cause contamination on composite surfaces when they are used for surface chemistry analysis. In this work, we explore an all solid-sate electrochemical sensor technology. Redox pairs or mediators are combined into a solid-state electrolyte, Nafion^{TM}. The mediators can pass electrons to or from the composite surfaces causing slight reduction or oxidation of the composite surfaces. The output current in response to cyclic polarization (cyclic potential scanning) is used as the indication of the surface contamination level.

The sensors included a working or sensing electrode with mediated Nafion clusters, Nafion membrane, Pt catalyzed carbon counter electrode, and Ag|AgCl reference electrode. The working electrode and counter electrode were attached to the Nafion membrane from different sides. The sensors were tested on different kinds of surfaces: original, polished, and sulfuric acid treated acrylic samples and pristine peel ply prepared, polished, and sulfuric acid treated composite laminate surface samples. The sensors showed a high sensitivity to the surface contamination. The performances and possible mechanisms related to the electrochemical sensors are discussed.

Acknowledgments

First of all, I would like to express my sincere appreciation to my advisor and friend, Dr. Xiangyang Zhou, for his guidance, encouragement and support during the entire course of my graduate studies at the University of Miami. I am deeply grateful and appreciative for all his help and guidance. Second, I would like to thank Shijie Tang for his help during my graduate study. I would like to thank the Department of Mechanical and Aerospace Engineering and Graduate School at University of Miami for their generous financial support. Finally, I am deeply grateful to my mother and father, who always encourage and take care of me selflessly. I am also deeply grateful to them, for their love and all that they suffered and suffer for me.

TABLE OF CONTENTS

LIST OF TABLES

LIST OF FIGURES

CHAPTER 1 Literature Survey

1.1 Bonded structures in aviation industries

Reducing the weight of components and systems is very important in aerospace engineering applications. It yields significant fuel savings which gives great financial incentives to airlines. Replacing mechanical fasteners with adhesive bonds is one of the most effective ways. The main advantages adhesive bonding provides are: a) light-weighted structure; b) joining different materials with dissimilar thicknesses without galvanic corrosion and distortion; c) joining heat-sensitive alloys d) producing bonds with unbroken surfaces; e) capacity of bonding small adherends; f) uniform stress distribution; g) higher fatigue endurance; h) smooth external surface; i) easiness for automation. In aviation industries, cost savings of 60% - 70% are realized in assembly processes via implementation of adhesive bonding technology [1]. Adhesive bonding is beginning to become the major technology for aviation industries.

Safety is a paramount issue of commercial aviation. However, the most significant bond failure related accident was the Aloha flight 243 case in Hawaii, April 28, 1988 [2], in which the bonded upper surface of the fuselage of a Boeing 737 separated in flight, leading to the death of one flight attendant. The aircraft landed with severe structural damage and a number of injured passengers. The structure had failed due to the coalescence of a number of small cracks (Multi-Site Damage). However, the reason that the cracks had occurred was due to the failure of an adhesive bond at the fuselage splice joint. The problem was the use of room temperature curing film adhesive, which had to be frozen to prevent premature curing. Condensed water on the surface inhibited the formation of chemical intermolecular bonds, leading to de-bonding in service and subsequent cracking. On 25 July 2003, another aircraft

accident happened and was investigated by BFU [3]. Although no one was injured, the aircraft was severely damaged. The bonding failed again and the conclusion stated by BFU was “The accident is to be attributed to deficiencies in the production of the wing and to an insufficient inspection.” The recommendation by BFU was “The Luftfahrt-Bundesamt should restrict operation of the aircraft type Duo-Discus until the sailplanes which may have defective bonding also are identified and inspected.” On July 23, 2004 [4], yet another major accident happened on a Fairey ritten Norman BN2A Mk III-2 ‘Trislander.’ The investigation identified two causal factors, one of them is ‘The de-icer boot separated due to peel stresses generated by forces on the propeller. The peel stresses arose due to physical damage or contaminations to the adhesive bond. During these years, there have been great improvements in FAA maintenance standards, increased inspections of airlines and more stringent airworthiness directives. However, there is still need to improve the ability to assure the quality, strength and durability of adhesive bonds.

1.2 Technology of adhesive bonding

1.2.1 General

Adhesive [5] is defined as a polymeric substance with visco-elastic behavior, capable of holding adherends together by surface attachment to produce a joint with high shear strength. Polymeric materials that fall within the categories of thermoplastics, elastomeric compounds, thermosetting resins and natural adhesives (animal glue, casein, starch, and resin) may serve adhesive functions.

Five mechanisms have been proposed to explain why one material is bonded to another: mechanical adhesion; chemical adhesion; dispersive adhesion; electrostatic adhesion and diffusive adhesion. Mechanical and chemical adhesions

provide the major strength of an adhesive bond. Adhesive bonding can be formed between metal to metal, composite materials to composite materials and metal to composite materials. Common adhesives used in aircraft structures include epoxies, acrylics, cyanocrylates and urethanes. Brand examples of epoxy adhesives and resins are Araldite™, Epibond™ and Epocast™.

1.2.2 Adhesion by mechanical interlocking

If a substrate has an irregular surface, then the adhesive may enter the surface irregularities prior to hardening. This simple idea gives the mechanical interlocking theory [6], which contributes to adhesive bonds with porous materials such as wood and textiles. An example is the use of iron-on patches for clothing. The patches contain a hot melt adhesive which, when molten, invades the textile material.

1.2.3 Adhesion by chemical intermolecular bonds

The chemical bonding theory of adhesion invokes the formation of covalent, ionic or hydrogen bonds or Lewis acid-base interactions across the interface [7]. Typical strengths of these are shown in Table 1, where they are compared with van der Waals forces which are the source of physical adsorption. The interactions are listed roughly in order of size, and it can be seen that the strongest are considerably stronger than the weakest. The ionic interactions have been calculated for an isolated pair of ions in a vacuum and those involving aluminum and titanium might occur when epoxide adhesives are used with these metals. Strengths of covalent bonds are typical for bonds of these particular types. It is a possibility that C-O bonds are formed when isocyanate adhesives are used on substrates with hydroxyl groups such as wood and skin.

Table 1 Typical strengths of chemical bonds and van der Waals interactions

Type of interaction	Energy kJ mol^{-1}
Ionic	
Na^+Cl^-	503
$Al^{3+}O^{2-}$	4290
$Tl^{4+}O^{2-}$	5340
Covalent	
C-C	368
C-O	377
Si-O	368
C-N	291
Hydrogen bond	
-OH-----O=C- (acetic acid)	30 ± 2
-OH-----OH (methanol)	32 ± 6
-OH-----N (phenol-trimethylamine)	35 ± 2
F^------HF	163 ± 4
F^------HOH	96 ± 4
Lewis acid-base	
$BF_3 + C_2H_5OC_2H_5$	64
$C_6H_5OH + NH_3$	33
$SO_2 + N(C_2H_5)_3$	43
$SO_2 + C_6H_6$	4.2
van der Waals forces	
dipole-dipole	≥ 2
dipole-induced dipole	0.05
dispersion	≥ 2

Hydrogen bonds involving fluorine are stronger than other types, and this is because fluorine is the most electronegative element. Here the values are taken from Jeffrey [8]. The data for Lewis acids and bases are actually enthalpies of mixing and are taken from Drago, Vogel et al [9].

1.2.4 Adhesives for aerospace application

There are two basic classes of adhesive bonding [7] in aerospace structures. One is structural bonding, with epoxy, phenolic, or acrylic adhesives, that transfers loads between members. The other is sealants, to protect against corrosion at interfaces. The stiffnesses of these classes of polymers differ greatly, but the two basic needs are remarkably similar. The first is that the adhesive or sealant will stay

stuck for the life of the structure, in all service and storage environments. Following is a list of adhesive systems.

- Epoxides

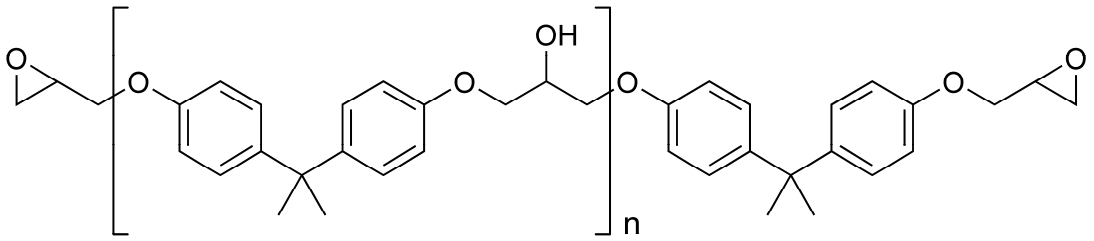

Figure 1 Commercial epoxy based on diglycidylether of bisphenol-A

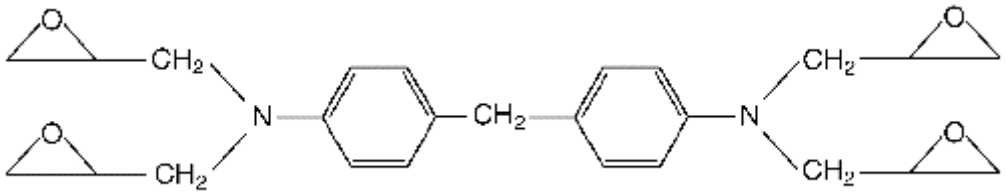

Figure 2 Tetraglycidyl diaminodiphenylmethane

The reaction of aromatic and aliphatic amines as hardeners with epoxide rings is shown below. The stoichiometry is that one epoxide ring will react with one amine-hydrogen atom in a condensation polymerisation.

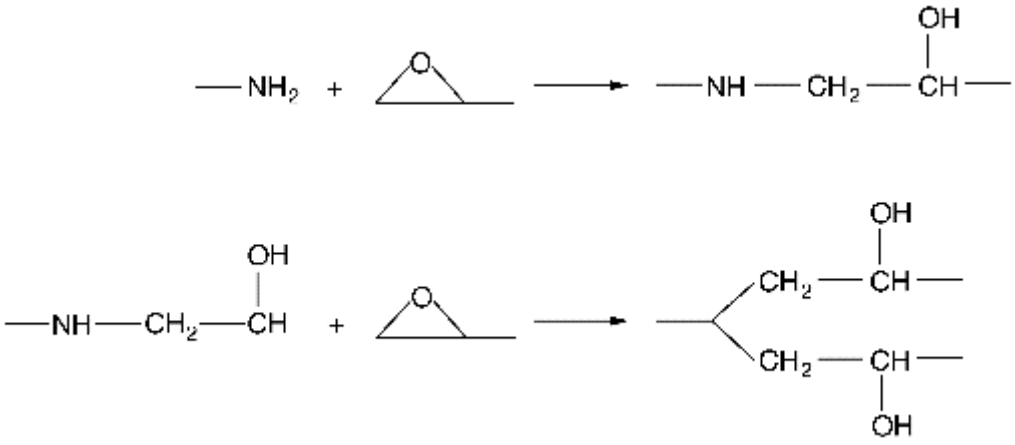

Figure 3 Reaction of primary amine with 2 epoxide groups

- Phenolic adhesives for metals

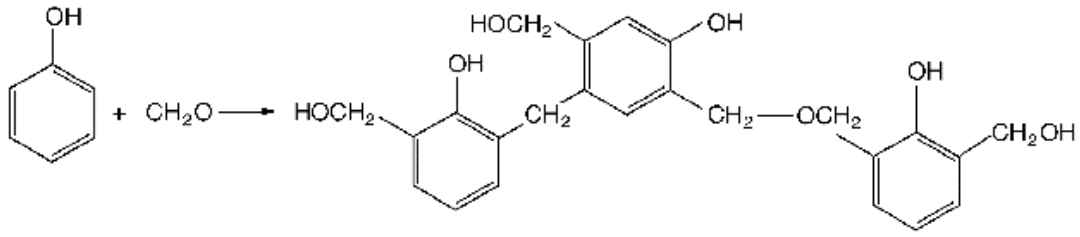

Figure 4 Reaction of phenol with formaldehyde to form a resole

- Structural acrylic adhesives

Table 2 Recipe of a structural acrylic adhesive

Component	Parts by weight
Methylmethacrylate	85
Methacrylic acid	15
Ethylene glycol dimethacrylate	2
Chlorosulfonated polyethylene	100
Cumene hydroperoxide	6
N.N-dimethylaniline	2

- Cyanoacrylates

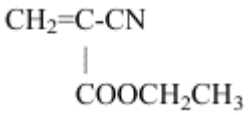

- Polyurethanes

-NCO + -OH = -NHCOO-
isocyanateol urethane

1.3 Degradation of adhesive bonding

1.3.1 Fracture

The basic principle for design of adhesive bonds is to design the joint such that the adhesive is always stronger than the unnotched strength of the adherends [10]. A design deficiency is characterized by fracture of the adhesive (cohesion failure). Processing deficiencies are usually characterized by interfacial failure

(adhesion failure) (Fig. 5) of the bond such that there will be areas where the adhesive remains on only one of the adherend surface, with the matching surface being free of adhesive, or by the presence of voids or other bonding defects in the adhesive. A good adhesive will only fail in cohesion failure mode.

Figure 5 Type of failure in adhesive bonds

1.3.2 Fatigue

The fatigue [11] phenomenon is common to most types of materials and it has been estimated that 80% of all engineering failures can be attributed to fatigue. The mechanisms of fatigue in polymers differ from those in metals, as will susceptibility to environmental factors such as moisture and temperature. Also, the visco-elastic nature of many polymers at modest temperatures will affect their response to cyclic stresses. The study of fatigue in bonded joints is further complicated by the fact that we are dealing with a heterogeneous system in which the adhesive itself is usually a composite material. Adhesive joints are generally considered to have good fatigue resistance compared with alternative joining techniques. This has been attributed to the reduction in stress concentrations, which deleteriously affect the fatigue life of metals. In addition, the adhesive layer prevents fretting fatigue, which may be a problem in mechanical joints. There is, therefore, a case for using adhesive joints in applications subjected to fatigue loading and hence the need to understand and predict fatigue in bonded joints.

1.3.3 Environment effects and durability

All adhesive absorb water [7]. Concerns over absorbed moisture and its removal from composite materials during structural repair are prevalent in several industries [12]. Adhesive layers in joints will absorb water and its vapour, and transmit it to the interface. This cannot be prevented by sealing the edges with a paint or lacquer, as these also absorb water. Once within a joint, there are several possible ways by which water may cause weakening. These have been reviewed by Comyn [13] and include the following.

- Altering the properties of the adhesive in a reversible manner, such as plasticisation
- Altering the properties of the adhesive in an irreversible manner, such as causing it to crack, craze or hydrolyse
- Attacking the adhesive-adherend interface
- Causing swelling stresses

The parameter which has created most interest in the literature is the work of adhesion in the presence of water, as this can be used to predict joint durability. Kinloch [14] has compared work of adhesion of adhesive interfaces in air and in water with their tendency to debond interfacially in an unstressed condition. Some data are shown in Table 3. The fact that interfacial debonding occurs only when the thermodynamic work of adhesion is negative is very strong evidence of the validity of hermodynamics in predicting the durability of adhesive bonds.

Table 3 Values of work of adhesion for various interfaces in dry air and in water

Interface	Work of adhesion/mJ m^{-2}		Interfacial debonding in water?
	Air	Water	
Epoxide/steel	291	-255	Yes
Epoxide/aluminum	232	-137	Yes
Epoxide/silica	178	-57	Yes
Epoxide/carbon fibre composite	88-90	22-44	No

Chemical bonds are inherently strong, and would usefully contribute to the durability of adhesive joints under environmental effects. Such bonds are formed between ion-pairs or via covalencies. The force F_{+-} of two ions separated by distance r is given by equation (1), where z_1 and z_2 are the valencies of the ions, e is the electronic charge, ε_0 is the permittivity of a vacuum and ε_r is the relative permittivity of the medium.

$$F_{+-} = \frac{z_1 z_2 e^2}{4\pi\varepsilon_0\varepsilon_r r^2} \tag{1}$$

Epoxide adhesives have low values of ε_r (about 4 or 5) and phenolics are probably similar, whilst that for water is about 80. Hence a small amount of water entering an adhesive would increase ε_r and lower F_{+-}, not to zero, but to a fraction of its original value. Complete removal of water would restore F_{+-} to its original value.

1.4 Surface pretreatments

Surface pretreatment is the most important process governing the quality of an adhesive bond [15]. It increases the bond strength by altering the substrate surface in a number of ways including [16]: *Increasing surface tension*, which increase the surface area and allow the adhesive to flow in and around the irregularities on the surface to form a mechanical bond; *Increasing surface roughness*, providing interlock adhesion,

or changing surface chemistry, which result in the formation of a chemical bond. For different adherends, pretreatment method varies. Table 4 gives affect of surface treatment on polymer composites [16].

Table 4 Effect of surface treatment on polymer composites

Treatment	Laser treatment	Flame treatment	Plasma treatment	Corona	Tear-ply	Acid etch	Abrasion and solvent wipe	Grit blasting	Peel-ply
Material	Thermoset and thermoplastic	Thermoplastic	Thermoplastic	Thermoplastic	Thermoset	Thermoset and thermoplastic	Thermoset and thermoplastic	Thermoset and thermoplastic	Thermoset
Nature of treatment	Ablation and/or oxidation	Oxidising	Ablation and/or oxidation	Oxidising	Remove mould release	Etch	Remove mould release	Remove mould release	Remove mould release
Surface tension		Y	Y	Y		Y			
Surface roughness	Y		Y		Y		Y	Y	Y
Surface chemistry		Y	Y	Y		Y			
Bond strength	Increase	Increase	Increase	Double	Increase	Slight increase	Increase found for thermosets	Increase found for thermosets	Increase
Durability			Good (90 days)	Good (90 days)	Good	Poor	Good for thermosets	Good for thermosets	Good
Ref.	[17]	[17]	[18]	[19]	[18]	[17]	[17]	[17]	[17]

The pretreatment methods are detailed as below:

- Peel-ply

an impregnated ply is removed immediately prior to bonding [20]

- Tear-ply

mainly used for thermoset composites as thermosets are reactive upon heating and hence do not require a chemical surface treatment [21]

- Grit blasting

gives strong and durable bond strength for thermosets but reveals very litter degree of success with thermoplastic materials [22]

- Abrasion/solvent cleaning

may be emplyed to degrease the surface and remove mould release agents from the adherend [23]

- Acid etching/anodizing

produces similar results to abrasion and grit blasting [24]

- Corona discharge treatment

exposes the substrate surface to excited atoms, ions and free radicals at atmospheric pressure. It increases surface tension and in some cases alters the surface chemistry by oxidizing the polymer matrix, which results in the increase in bond strengths [19]

- Plasma treatment

low-pressure plasma gas, which is electrically conductive and consists of excited atoms, ion and free radicals. Allows polymer surfaces to be cleaned, etched or chemically modified [21]

- Flame treatment

improves printability and paintability, by introducing oxygen containing

functional groups to the surface. Oxidizes the surface of the specimens [25]

- Laser treatment

produces high-strength adhesive bonds [26]

1.5 Formation of adhesive bond and surface chemistry

Many types of surface pretreatments result in a layer of uniformly distributed active sites, as evidenced by a profile of O- or N-containing functional groups (anchor groups) near the surface. Lone electron pairs on O- and N-containing groups could be donated to accepters (such as C-) to form covalent bonds. Because of abundant electron acceptors and anchor groups on the curing surface of adhesive, covalent bonds could link the adhesive and adherend together during curing of adhesives (Fig. 6). These covalent bonds at the interfaces are the major load transfer mechanisms between the adherends.

Adhesive-bonded joints based on covalent bonds are less susceptible to the effect of the surface contamination or water ingress due to high bond energies of covalent bonds (Table 1). Olsson-Jacques et al. [27] studied the effects of Avtur fuel on the durability of epoxy adhesive bonds with aluminum adherends. They found that hydrocarbon contaminants affect bonding strength only before the formation of covalent bonds between a primer (SCA) and the substrate. Rider and Arnott [28] compared the effects of different primers against the water ingress to the bonded epoxy-aluminum joints. Their results indicated that water ingress was retarded by forming dense covalent bonds between the adhesive and substrate with a silane primer as the coupling agent.

In summary, it is very important that a pre-bonding surface treatment process should result in contamination free and chemically active (with O- and N- groups)

adherend surface to ensure an adhesive bond with a desired high strength and durability.

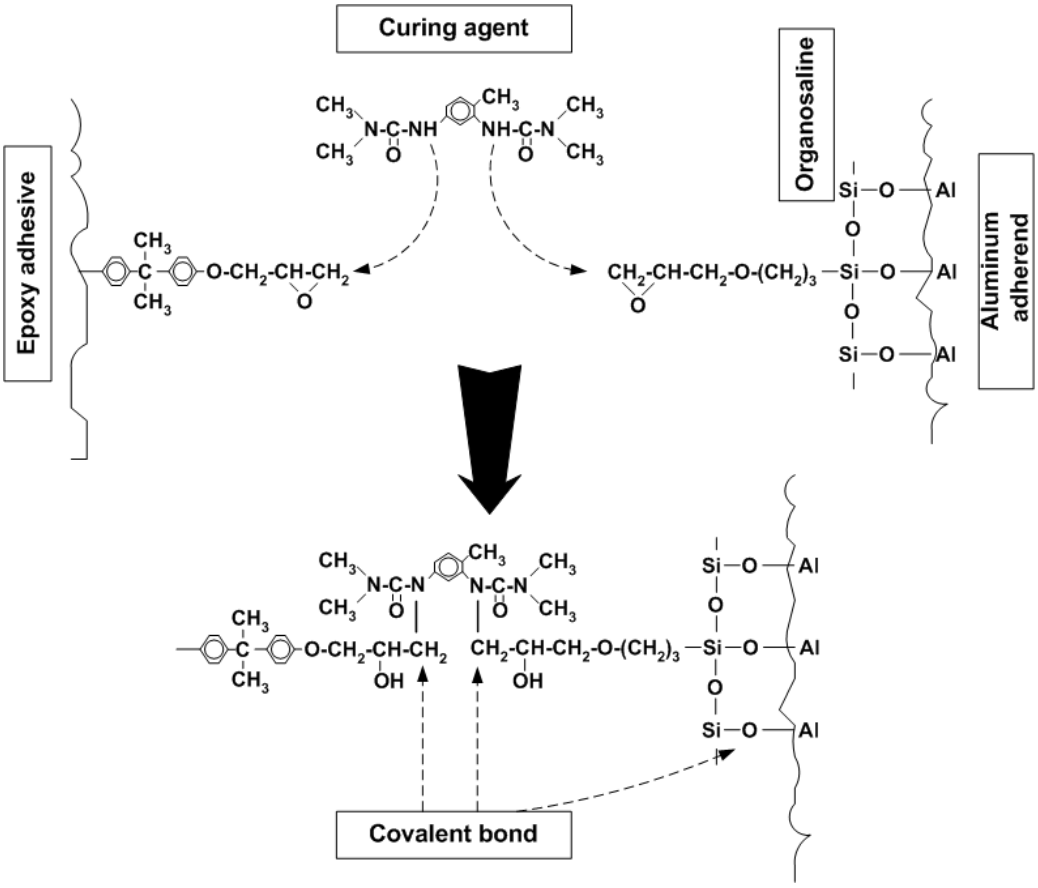

Figure 6 Covalent bond formation between adherend and adhesive

1.6 NDI and NDT methods used in aviation industry

Traditionally, destructive tests such as lap shear and Boeing wedge tests have been used to determine bond strength. These tests are fine for gauging the properties and strengths of a particular pre-treatment or adherend-adhesive composition, but these tests are destructive and cannot provide an online, in-field evaluation of the pre-bonding adherend surfaces. Other NDI methods are being used in aircraft manufacture processes and they listed as follows.

1) Contact angle

Following the well known Young Equation [29]:

$$\gamma_{sv} = \gamma_{sl} + \gamma_{lv}\cos\theta \quad (2)$$

representing the equilibria established by a sessile drop on a solid surface, a contact angle (θ), as in Fig. 7 represents the angle of the tangent of the drop at the triple point between solid, liquid, vapor and the free energy of the solid substrate γ_{sv}, and the interfacial free energy of the liquid and solid γ_{sl}. The surface free energy, or surface tension, of the liquid γ_{lv} will be known and θ provides a readily observed manifestation of the interaction of a liquid with a solid. Thus, if we consider water as the wetting liquid, a high surface energy substrate such as an oxide will wet fairly readily.

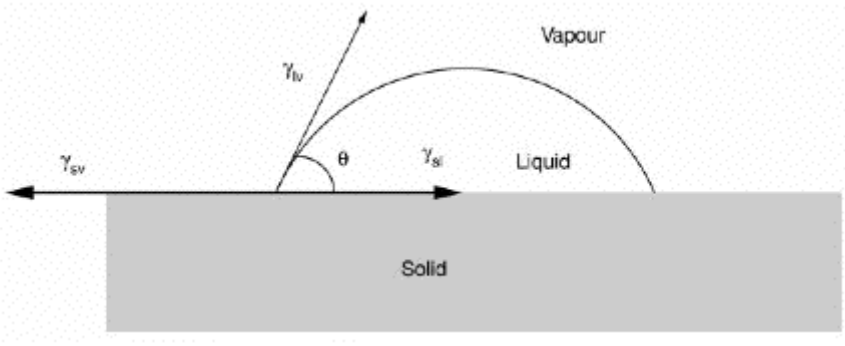

Figure 7 Thermodynamic equilibria of a sessile liquid drop on a solid substrate

2) Neutron radiography

NR is one of the most commonly used NDE methods used for inspecting adhesive joints in aircraft structures [30]. Its principle is similar to X-ray radiography. The difference is X-rays interact with the electron cloud surrounding the nucleus of an atom, neutrons interact with the nucleus itself. Moisture and corrosion were found in the honeycomb structure and hydration found in composite and adhesive layers by

NR. While voids, cracks and damaged honeycomb sections could be found by X-radioscopy.

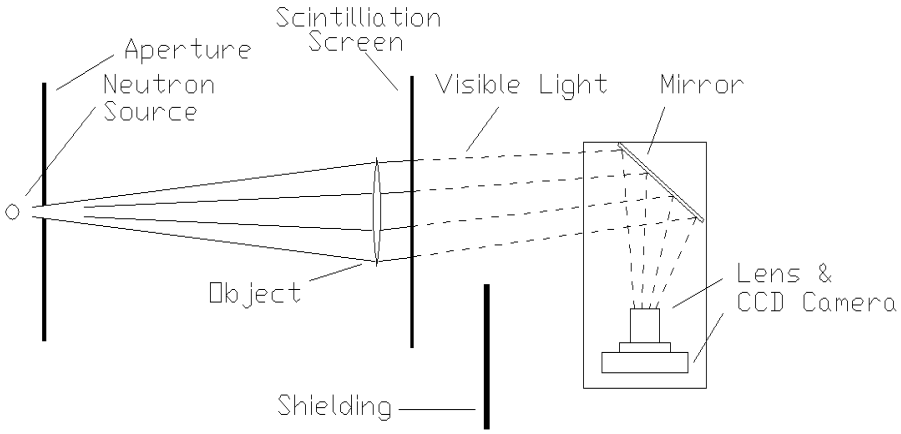

Figure 8 Basic components of a NR system

3) X-ray and gamma ray

X-radiation [31] is a quantitative spectroscopic technique that measures the elemental composition. X-ray photoelectron spectroscopy (XPS)are obtained by irradiating a material with a beam of aluminum or magnesium X-rays while simultaneously measuring the kinetic energy (KE) and number of electrons that escape from the top 1 to 10 nm of the material being analyzed. XPS requires ultra-high vacuum (UHV) conditions. It detects all elements between Z=3 to Z=103 and it cannot detect hydrogen or helium.

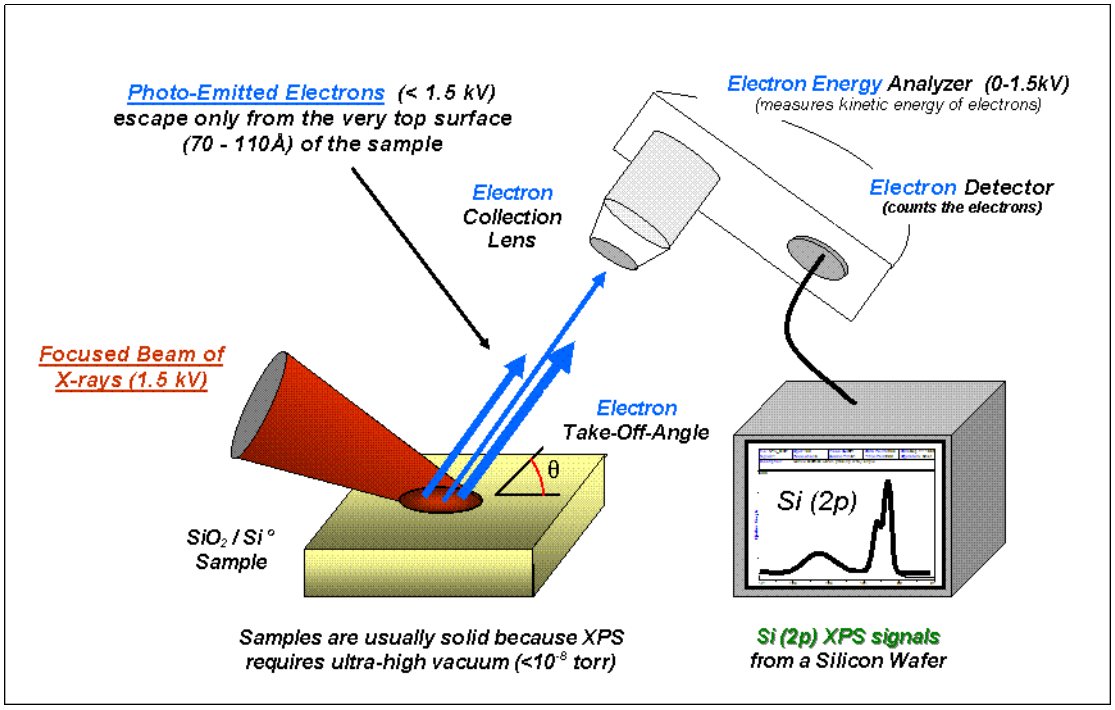

Figure 9 Basic components of a monochromatic XPS system

4) Near-infrare

The general setup for transflectance measurements is such that the incident light passes through the sample of interest, reflects off for example an aluminum plate, and then travels back through the sample before reaching the detector.

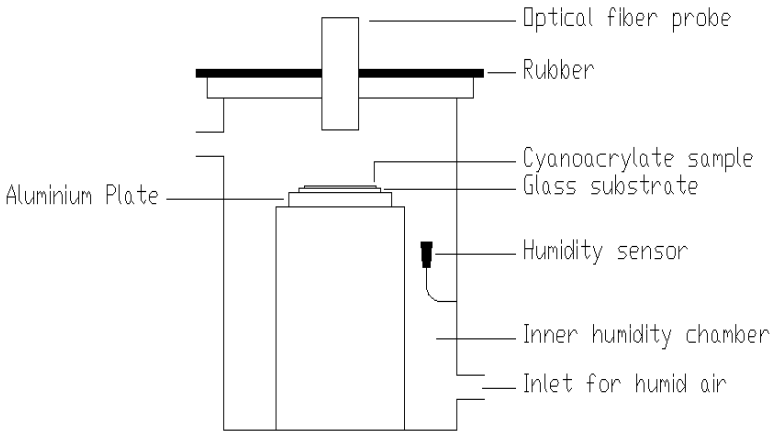

Figure 10 Basic components of a NIR system

It is possible to analyze the complex reflection spectra of near infrared waves to determine the quality of an adhesive bond. Tomlinson et al. [32] used optical fibers to fire light at the specimen which had an aluminum plate placed behind it as shown in Fig. 10. There are problems with penetration into thick parts and assemblies, whilst resolution also remains poor.

5) Non-linear ultrasound (NLUS)

Significant NLUS arises when a high amplitude ultrasound wave causes a local mechanical deformation of a sample, leads to non-harmonic components in the transmitted ultrasound pulse, which are detected as overtones by Fourier analysis. With rising ultrasound amplitude the non-linear deformation range in the adhesive metal bond is reached first in the weakest region of the adhesive polymer.

Bockenheimer et al [33] investigated the possibilities of inspecting structural adhesive bonds using ultrasound waves. Fig. 11 shows a simplified overview of their set-up.

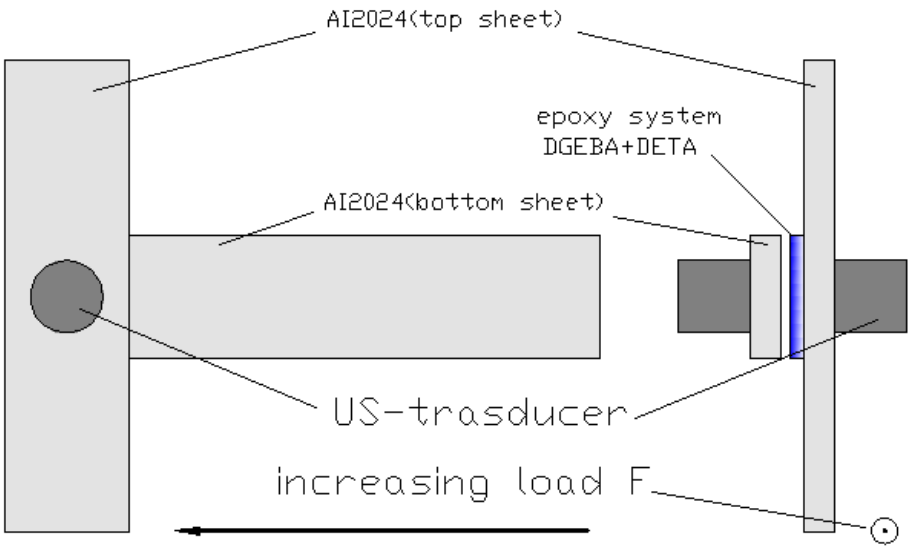

Figure 11 Basic components of a NLUS system

6) Transient thermal NDT

Thermography [34] thermal imaging, or thermal video, is a type of infrared imaging. Thermographic cameras detect radiation in the infrared range of the electromagnetic spectrum (roughly 900–14,000 nanometers or 0.9–14 μm) and produce images of that radiation. Since infrared radiation is emitted by all objects based on their temperatures, according to the black body radiation law, thermography makes it possible to "see" one's environment with or without visible illumination.

7) Electrical potential

DC potential drop technique [35]: a constant DC current is passed through the specimen. The electrical voltage is measured across the crack mouth and is related to the crack length. The electric potential across the crack mouth can be related to the unbroken crack ligament resistance, R, through the Ohm's law:

$$V = IR \tag{3}$$

For the specimen shown in the Figure 12, the cross-sectional area of the specimen can be calculated from the measured resistance. With respect to a crack through a material of uniform thickness, the change in un-cracked length can be calculated from

$$L = L_0 \frac{R_0}{R} \tag{4}$$

where L_0 and R_0 are the initial crack length and resistance of the un-cracked ligament respectively.

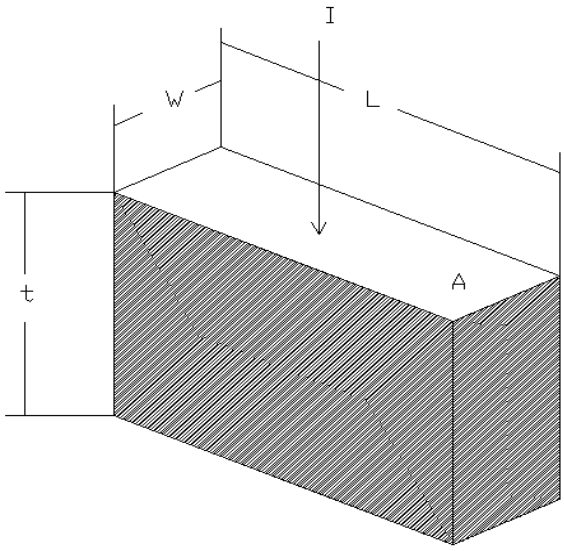

Figure 12 Resistive element for electrical potential evaluation

8) Electrical impedance spectroscopy (EIS)

EIS [36] works by creating a parallel circuit which can be used to compare the "capacitance" and conductance of a component. At certain low amplitudes, the impedance becomes independent of frequency. EIS can detect corrosion and absorption of moisture in polymeric systems and can even detect moisture ingress in coated metals which is obviously a precursor to corrosion of the substrate.

1.7 No technology available for in-field surface chemistry analysis

It is clear that all the existing methods have their limitations. None of them can provide in-field surface contamination detection for pre-bond surfaces. As a result, there is no method satisfies the requirement for online and in-field surface chemistry analysis that specified by the FAA (Federal Aviation Administration). Because of lack an in-field surface chemistry analysis method, the aviation industry relies on a complicated and tight procedure controls to ensure the quality of the pre-treated surfaces. This involves a number of Standard Operation Procedures (SOPs)

and certifications including composite material, adhesive, equipment, procedure, environment, and technician certifications. Without a definitive surface chemistry analysis method, the SOPs and certifications may result in excessive efforts and costs or insufficient quality of the pre-bond surface. The advantages and disadvantages of the NDT and NDI methods as for surface chemistry analysis are listed Table 5.

Table 5 Advantage and disadvantage of NDT

Method	Advantage	Disadvantage
Contact angle	Easy to apply and can detect surface energy	Cannot detect surface contamination
Neutron radiography	Detect surface contamination	Bulky and complex equipment
XPS	Detect surface contamination	High vacuum needed
NIR	Less complex system	Poor resolution
NLUS	Detect voids and cracks	Cannot detect surface contamination
Thermography	Rapid evaluate large area, data highly interpretable	Cannot detect surface contamination
Electrical potential	Analyze metal/composite bonds with a simple device	Cannot detect surface contamination
Electrical Impedance spectroscopy	Analyze metal/composite bonds with a simple device	Cannot detect surface contamination

CHAPTER 2 Introduction to Solid-State Electrochemical Sensor

2.1 Need for in-field surface inspection technology

Adherend surface preparation is a critical issue to structural integrity of bonded structures. Inadequate surface roughening, possible chemical contamination on peel ply, released fabric and released film and surface water moisture result in poor adhesion, i.e. a weak bond between the adhesive and adherend, and reduced long-term durability [37-40]. The problems with chemical contaminations from peel ply, release fabric and release film that prevent adhesion of the adhesive to the substrate are now fairly well known. What is far less understood is the adverse influence of pre-bond water moisture that is unable to avoid during manufacture, repair, and service. Water inclusion in pre-bond adherands could affect short-term or long-term strengths of adhesive bonding depending on how fast are the diffusion and accumulation processes [41-42]. As being presented in the recent FAA meeting on bonding structures, water moisture is claimed as one of the most adverse factors in adhesive bonding processes [43]. The pre-bond surface preparation is acknowledged as the most important factor in adhesive bonding processes. Solvent wipe, grit blast, peel ply and gas plasma treatment are the common practices of bond surface preparation. As the term suggests, peel ply practice employs tear films. The tear film remains in place until the adhesive is applied. It is then removed together with surface contaminants. However, the peel ply process introduces release agents that again reduce bond adhesion to the bond surface [10,44,45].

Current adhesive bonding quality assurance practice relies on tightened surface preparation process control and mechanical testing on bonded specimens and non-destructive inspection (NDI) after bonding [10,37,44-46]. The mechanical testing methods used by the aircraft manufacturers to assess individual bonded panels are

based on component or coupon test pieces representing the bonded structure and routine standard shear and peel test pieces. Many of these tests have been based on ASTM D1002 Lap-Shear Strength tests and D1876 Peel Strength Tests, though it is claimed [10,37,44,45] that the most appropriate test for evaluation of surface preparation is the Boeing Wedge Test, i.e. the ASTM D3762 test. In addition to the stress-based methods mentioned above, fracture mechanics and fatigue approaches have been developed and used to evaluate the strength and environmental durability of bonded structures [47]. One of the major drawbacks of these mechanical testing methods is that they are carried out on small specimens, not on the actual prepared surface for bonding. As such, these tests have been found to be inadequate to ensure bond quality. A number of non-destructive inspection (NDI) methods including conventional ultrasonic techniques, oblique incidence ultrasonic technique, Lamb waves, sonic vibrations, spectroscopic methods, acoustic emission, thermal methods, radiography, and optical holography, have been used to detect defects in adhesive bonded structures [10,38,39,45]. While these NDI tests will eliminate bonds with obvious defects and cracks, they do not provide assurance of bond strength and long-term durability. Good bond quality must be obtained by management of all aspects of the bonding process during production. Thus, in the absence of a definitive surface quality control method, laborious and sometimes inadequate measures are used to ensure the quality of adhesive bonding, thereby creating an undue expense on an otherwise economic manufacturing process.

X-ray photoelectron spectroscopy (XPS), ion scattering spectroscopy (ISS), Auger spectroscopy (AES), secondary ion mass spectroscopy (SIMS), X-ray fluorescence spectroscopy (XRF), Fourier transform infrared spectroscopy (FTIR), and scanning probe microscopy (SPM) are commonly used as surface contamination

evaluation methods [38,39]. Recent technical developments have enabled a number of portable chemical analysis technologies including portable XPS and XRF. Although these portable chemistry spectroscopy methods can provide definitive information of composition, structure, and quantity of surface contaminates, like the mechanical tests, they can't be conveniently employed for chemistry analysis on the actual bonding surface areas of large components. Contact angle method [48] has been employed for field surface analysis, however they do not quantify the surface chemical composition. The Federal Aviation Administration (FAA) has found that these methods are inadequate to determine whether the actual component surface preparation is acceptable. This calls for a convenient, definitive method to detect the contaminants and water moisture on pre-bond adherend surface.

Electrochemical sensing technology includes a varieties of devices based on conductimetry, polarization measurement, cyclic voltammetry, electrochemical impedance spectroscopy (EIS) and electrochemical noise analysis (ENA). Electrochemical sensing technology just needs a small input energy density (<0.1 mW cm^2). Many electrochemical humidity sensors are based on conductimetry. One of the most promising sensors for water moisture detection is the four-probe electrochemical cell that is fabricated using water sensitive conductors such as carbon powder (electron conductor) and proton conducting polymer electrolyte (PCPE) (proton conductor) [49,50]. Electrochemical impedance spectroscopy (EIS) and ENA technologies have been used to detect water ingress or accumulation at the interfaces between polymer and metallic components [51,52]. Stripping electrochemical sensors (SESs) [53] technology utilizes the fact that specific atom or molecule is oxidized at a specific voltage at a specific reaction rate. This allows spectral analysis of composition and quantity of surface contaminates. However, classical electrochemical

sensors with liquid electrolytes are usually rather bulky and awkward. Moreover, leakage of the electrolyte may corrode the device and contaminate the studied composite component. In addition, traditional electrochemical sensors cannot be used to analyze the surfaces of inert polymer materials including polytetrafluoroethylene (PTFE), acrylics, and expoxides.

2.2 Electrochemical reactions on polymer materials via mediation

2.2.1 Hydrocarbon based polymers

The difficulties of rendering surface oxidation by exposing the polymer to an anodically polarized electrode or to some soluble reactive, anodically generated oxidizing agent are as follows: Firstly, the oxidation potentials of saturated hydrocarbons are very high so that the electrolytes used tend to be oxidized instead of the polymer. Electrolytes resistant to oxidation at these very high anodic potentials tend to be expensive and extremely unpleasant typically consisting of mixtures of fluorosulphonic acid with anhydrous antimony pentafluoride, the so called super acids [54, 55]. Secondly, it is unlikely that the treated polymer surface is an electronic conductor so that an anodic oxidative process proceeding from a single point contact anode can be ruled out. Using an electrochemically generated oxidizing agent as a mediator it should be possible to overcome these problems as shown schematically below:

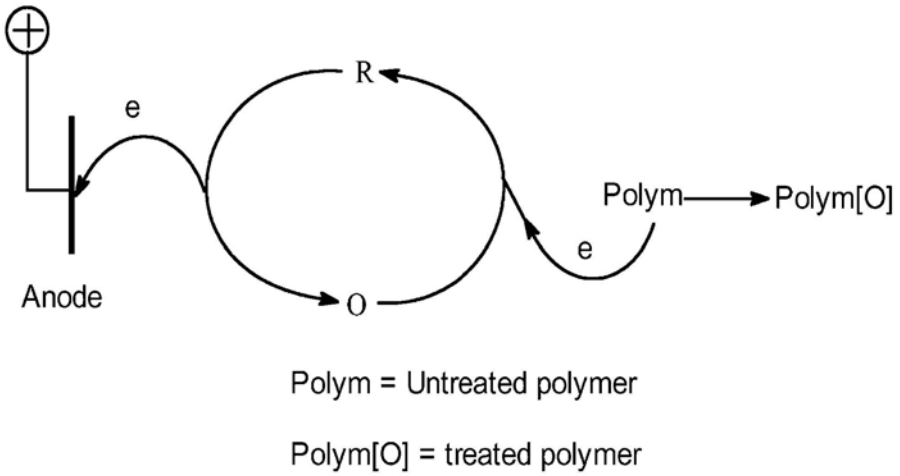

Figure 13 Schematic of the mediated electrochemical oxidation of a polymer

R represents soluble species that can be reversibly oxidized at an anode to yield an oxidized species O that in turn is capable of oxidizing the polymer surface being reduced back to R in the process. Water soluble reversible redox couples for the role of mediator include Ce(IV)/Ce(III) E_0 =1.72V; Co(III)/Co(II) E_0 =1.83-1.92V and Ag(II)/Ag(I) E_0 =1.98V. Ag(II)/Ag(I) was chosen as its high E_0 value, its effectiveness as an oxidant for many classes of organic compounds and its fast electrode kinetics at a platinum anode with a standard charge transfer rate constant in dilute nitric or perchloric acids [56]. Electrochemically generated silver (II) nitrate was capable of attacking the surface of saturated polymers such as polyethylene (PE) and polypropylene (PP) as well as those of unsaturated/aromatic polymers.

2.2.2 The mechanism of the silver (II) oxidation of Polyethylene (PP) and high-density polyethylene (HDPE)

The direct electrochemical oxidation of aliphatic hydrocarbons takes place at high overpotentials and requires the use of non aqueous and generally very highly acidic electrolytes [56, 57]. However, aliphatic hydrocarbons including PP and PE are

oxidized by aqueous solutions of transition metal ions including Co (III), Ce (IV), Mn (VII) and Cr (VI). [57]. According to Wiberg [58], the oxidation of a number of hydrocarbons by chromic acid proceeds by initial formation of the alkyl radical which then undergoes further one electron oxidation steps to yield the chromium(IV) ester followed by its hydrolysis to the alcohol which in turn is oxidized further to the corresponding carbonyl compound. The mechanism of the silver (II) oxidation of benzene has been presented as proceeding via hydroxyl radicals presumably produced by silver (II) oxidation of water [59]. According to Paire et al. [60] Aliphatic hydrocarbons are not oxidized by solutions of silver (II) nitrate in the absence of the polarized anode. These authors suggest that the reaction is initiated by short-lived nitrate radicals generated by the anodic oxidation of nitric acid. This is clearly not the case in the silver (II) mediated oxidation of polymer surfaces which take place both in the presence and absence of the polarized anode. Brewis and Dahm put forward the suggestion [61] that in the case of PP and HDPE surfaces the $AgNO_3^+$ ions directly attack exposed carbonhydrogen bonds of the relatively conformationally rigid polymer chain to yield initially an organo-silver ion which then undergoes oxidative elimination to a carbonium ion which in turn rapidly hydrates to yield the alcohol as shown in below.

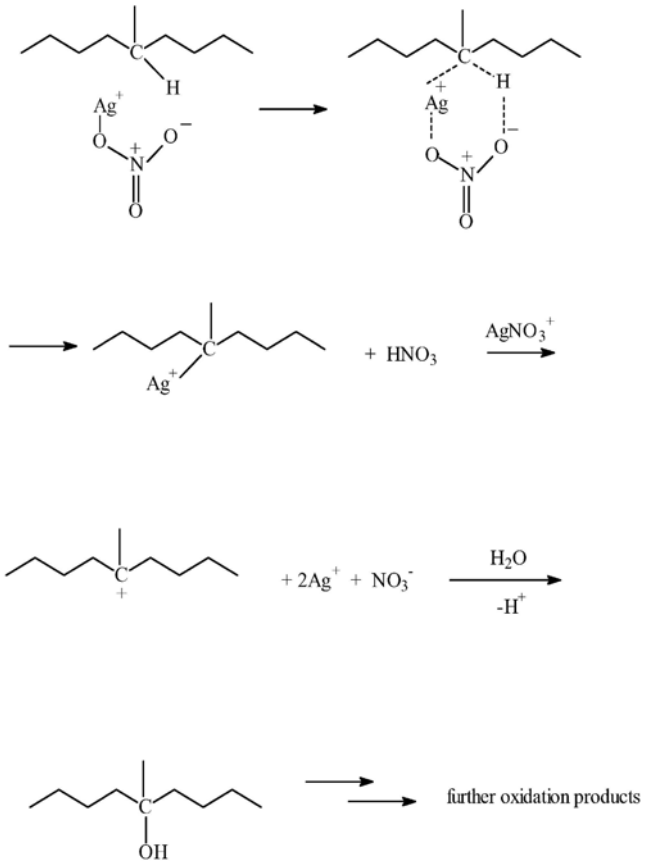

Figure 14 Mechanism of the silver (II) oxidation of polyolefins

Such a mechanism would be sterically demanding and the more accessible CH_2 groups of HDPE could be attacked in preference to the more hindered groups of PP. The fact that the amount of oxygen that can be introduced into the surface is limited to about 10% for HDPE and 5% [62] for PP even for prolonged treatment times may be due to the presence of a limited number of reactive centers on the polymer surface and/or to chain scission brought about by further rapid and complete oxidation of a particular polymer chain once functionalized. Experiments on low molecular weight model compounds showed that simple aliphatic alcohols, ketones alkenes, etc. react much more rapidly with silver (II) nitrate than the corresponding parent hydrocarbons [61]. It appears that once the polymer has become functionalized further oxidation takes place rapidly by further reaction of the functional groups resulting ultimately in complete mineralization of the organic species. The surface concentration of oxygen

2.2.3 Mechanism of redox mediation

Redox mediation phenomenon [62] is about a substance of low conductivity in contact with a metal on one side, and the other side contact with a solution containing one or both component of a redox couple on the other side, capable of mediating electron transfer between the redox couple and the metal. Redox mediators are substances containing redox centers which are electroactive, when in contact with a metal and forming part of a suitable electrochemical cell can be oxidized and reduced. Examples of redox mediators are electroactive polymers. Electroactive polymers are classified in redox and conjugated polymers. The first ones possess, either as a part of the monomer unit or as a coordination compound, chemical groups that are the ones participating in the redox reaction.

The redox mediation phenomenon has several review treating these matters [63,64], and theoretical treating of current-potential response during redox mediation [65-68].

Important applications of redox mediation are in the field of electrocatalysis [63,64], membrane [65-68], sensors and battery electrodes [69].

Several models have been developed to explain some of the facts mentioned above. Most of them employ the limiting current as the only criteria to determine the rate determining step. Other treatments concentrate on the process at the metal/polymer interface [66,68]. Only a few workers treated the complete voltammetric curve [65,66]. However, none of these treatments included two facts that are present in this phenomenon: (i) the presence of a potential difference at the polymer solution interface and (ii) the fact that the redox mediation reaction is actually a heterogeneous electron transfer reaction.

Considering a system formed formed by an electronic conducting electrode

(Au, Pt, glassy carbon, etc.) coated with a redox polymer in contact with an electrolytic solution [70]. The coated electrode is forming part of an electrochemical cell so its potential can be precisely controlled. An electrochemical reaction takes place at the electrode/polymer interface between the oxidized and reduced forms of the redox sites in the polymer, α and ρ:

$$\rho = \alpha + e \tag{5}$$

Charge is transported within the mediator by electron hopping, a process that can be described as a diffusion one.

The polymer coating is in contact with a solution containing a redox couple, O/R, where O is the oxidized form and R the reduced one. A redox reaction (the mediation reaction) takes place at the polymer/solution interface:

$$\rho + O = \alpha + R \tag{6}$$

The mediation reaction is a charge (electron) transfer reaction. We will assume that reaction (6) involves one electron.

In the solution, species O and R are transported to and from the polymer/solution interface. In steady state conditions, this is usually carried out by controlling the fluxes of O and R employing a rotating disk electrode (RDE) [71].

Under a constant applied potential to the electrode, the system reaches a steady state, then, all the species involved reach stationary concentration profiles. Under these conditions, there are not net ionic currents at the polymer/solution interface and the current at this interface is entirely due to the electron transfer of the mediation reaction.

The kinetics of the redox mediation process involves several steps:

(i) the charge transfer at the electrode/polymer interface,

(ii) charge transport within the polymer,

(iii) electron transfer at the polymer−solution interface,

(iv) mass transfer to and from the bulk of the solution.

These different steps are schematically shown in Fig. 15.

Murray et al. derived a general i–E relationship for the redox mediation in the cases in which reactants O and R in solution cannot penetrate inside the film and linear concentration profiles within the mediator film are achieved in the steady state. The characteristic mass transport and charge transfer coefficients, expressed as currents are given by:

$$i_{k,a} = FAk_a C_T C_{R,s} \tag{7}$$

$$i_{d,R} = FAk_{d,R} C_{R,s} \tag{8}$$

$$i_e = FAk_e C_T \tag{9}$$

$$i_{k,c} = FAk_a C_T C_{O,s} \tag{10}$$

$$i_{d,O} = FAk_{d,O} C_{O,s} \tag{11}$$

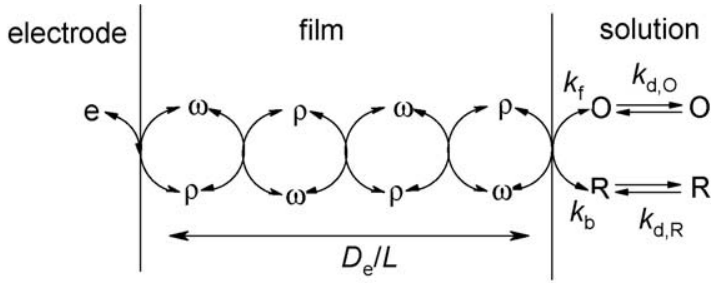

Figure 15 Different steps taking place during the redox mediation process. The transport of species in solution is characterized by the mass transfer constants $k_{d,O}$ and $k_{d,R}$; the kinetic of electron transfer at the polymer/solution interface by k_c and k_a and the electron transport in the polymeric film by the quotient between the electronic diffusion coefficient and the film thickness, D_e / L

2.3 Nafion^{TM}-solid state electrolyte

Adding mediators or redox electron carriers in liquid electrolyte can effectively enable electrochemical reactions on polymer surface. However, the use of a liquid electrolyte on prebonding composite surfaces result in contamination. The availability of Nafion solid electrolyte provides an opportunity for designing all solid-sate electrochemical sensors that can detect contamination of on polymer or composite surfaces via electrochemical potentiostatic measurements or cyclic voltammetry measurements. Nafion [72] is a sulfonated tetrafluorethylene copolymer discovered in the late 1960s by Walther Grot of DuPont de Nemours.[73] It is the first of a class of synthetic polymers with ionic properties which are called ionomers. Nafion's unique ionic properties are a result of incorporating perfluorovinyl ether groups terminated with sulfonate groups onto a tetrafluoroethylene (Teflon) backbone [74] (Fig. 17). Nafion has received a considerable amount of attention as a proton conductor for proton exchange membrane (PEM) fuel cells because of its excellent thermal and mechanical stability.

2.3.1 Structure

The first model for Nafion, called the Cluster-Channel or Cluster-Network Model, consisted of an equal distribution of sulfonate ion clusters (also described as ‘inverted micelles’) with a 40 Å (4 nm) diameter held within a continuous fluorocarbon lattice. Narrow channels about 10 Å (1 nm) in diameter interconnect the clusters, which allow transport hydrogen ions or protons.

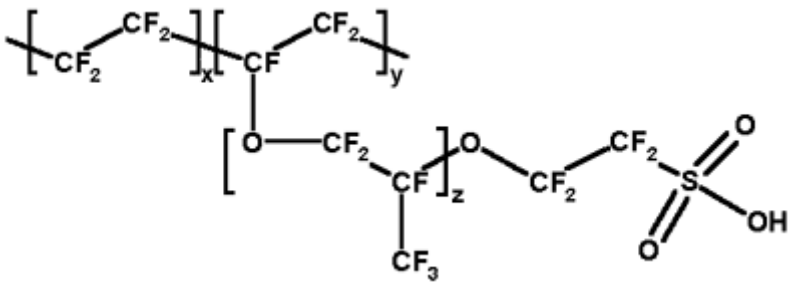

Figure 16 Molecular structure of Nafion

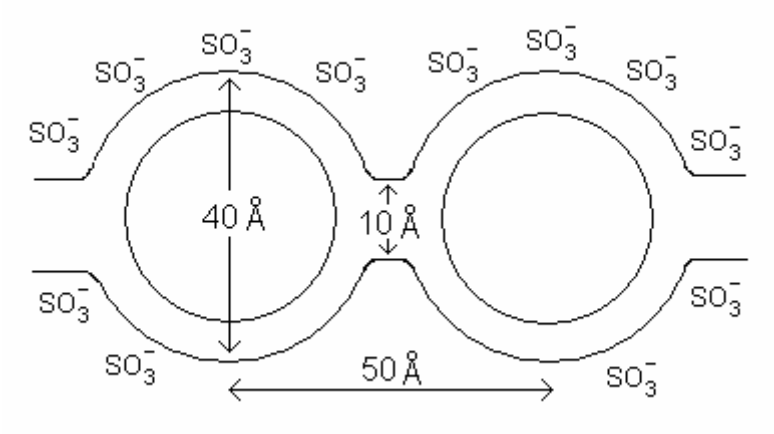

Figure 17 Nafion cluster network model

2.3.2 Property

- It is highly conductive to cations, making it suitable for many membrane applications.
- It resists chemical attack. According to DuPont, only alkali metals (particularly sodium) can degrade Nafion under normal temperatures and pressures.
- The Teflon backbone interlaced with the ionic sulfonate groups gives Nafion a high operating temperature, e.g. up to 190 °C.
- It is a super-acid catalyst. The combination of fluorinated backbone, sulfonic acid groups, and the stabilizing effect of the polymer matrix make Nafion a

very strong acid, with pKa ~ -6. In this respect Nafion resembles the trifluoromethanesulfonic acid, CF_3SO_3H, although Nafion is a weaker acid by at least three orders of magnitude.

- It is selectively and highly permeable to water. The degree of hydration of the Nafion membrane directly affects its ion conductivity and overall morphology.

2.4 Objective of research

The discovery of the mediated electrochemical cell and the availability of Nafion solid electrolyte provide an opportunity to develop an all sold-sate electrochemical sensor that can be used to detect the chemical properties or contaminations of the composite surfaces. It is thus of great interest to conduct a feasibility study of a solid-state electrochemical sensor for surface chemical analysis. Electrochemical analysis gives the idea of surface oxidation situation.

CHAPTER 3 Experimental Procedure

3.1 Design of the solid-state electrochemical sensor

The design of the electrochemical sensor is illustrated in Fig. 18. The sensor consists of a porous Ag electrode as the working or sensing electrode. The electrode also contains Nafion clusters impregnated with mediators. The sensing electrode is intimately in contact with the surface of a sample that is going to be analyzed. The working electrode and the counter electrode sandwich a piece of Nafion membrane. An Ag|AgCl electrode is placed on the counter electrode side. These components form an all solid-state electrochemical cell. An electrochemical measurement system is used to enable a polarization of the working electrode resulting oxidation or reduction of the surface. The extent and characteristics of the cyclic voltammetry may reflect the surface chemistry or contamination level.

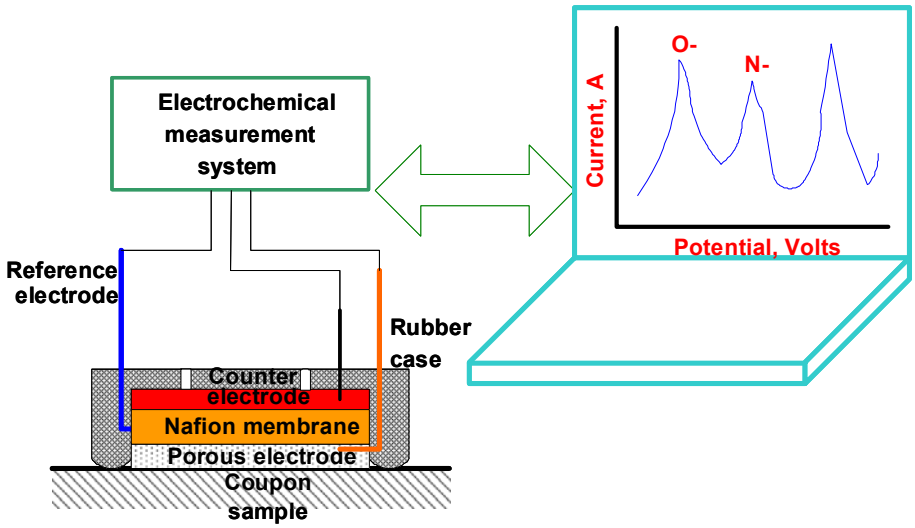

Figure 18 Schematic of the solid-state electrochemical sensor

Working electrode of the sensor

The basic procedure for preparation of the working electrode is listed below:

1. A square 2 cm by 2 cm piece of silver gauze was cut as the electrode.
2. An electrochemical deposition method was used. An electrochemical deposition bath contained saturated AgNO3 and 1 M HNO3. An electrical power source was used to provide an appropriate voltage and current. A 0.2 V voltage was applied for 2-4 minutes between the Ag gauze and a Pt wire that was used as a counter electrode. The Ag gauze was then immersed in a Nafion solution (Liquion^{TM}). When the solvent (mainly isopropanol) is vaporized, the Ag gauze was placed in the saturated AgNO3 solution again for electrochemical oxidation and impregnation. These steps were repeated several times.
3. The coated Ag gauze was washed with deionized water and then dried.

Counter electrode of the sensor

1. A square 2 cm by 2 cm piece of carbon cloth or carbon paper was used as the electrode.
2. Activated Pt catalysts (40% Pt on carbon, Alfa Aesar) were mixed into a Nafion ionomer solution (Alfa Aesar).
3. The mixture was loaded on to carbon cloth. The counter electrode was wired used an Ag wire.

Reference electrode

The reference electrode was a piece of Ag gauze (1 cm x 1 cm) that was coated with AgCl:

1. An original Ag gauze was immersed into saturated HCl solution.

2. A 0.3 V voltage was applied between the Ag gauze and a Pt wire for a period of 2 minutes.
3. The resulting coated Ag gauze was washed with deionized water and dried.

Sensor assembly

1. The working electrode was attached to one side of a piece of Nafion 117 proton conducting membrane whereas the counter and reference electrode was attached the other side.
2. The electrodes were hot pressed using a hot press machine. The pressure for pressing was 1500 psi and temperature was 100°C. The entire procedure is illustrated in Fig. 19.

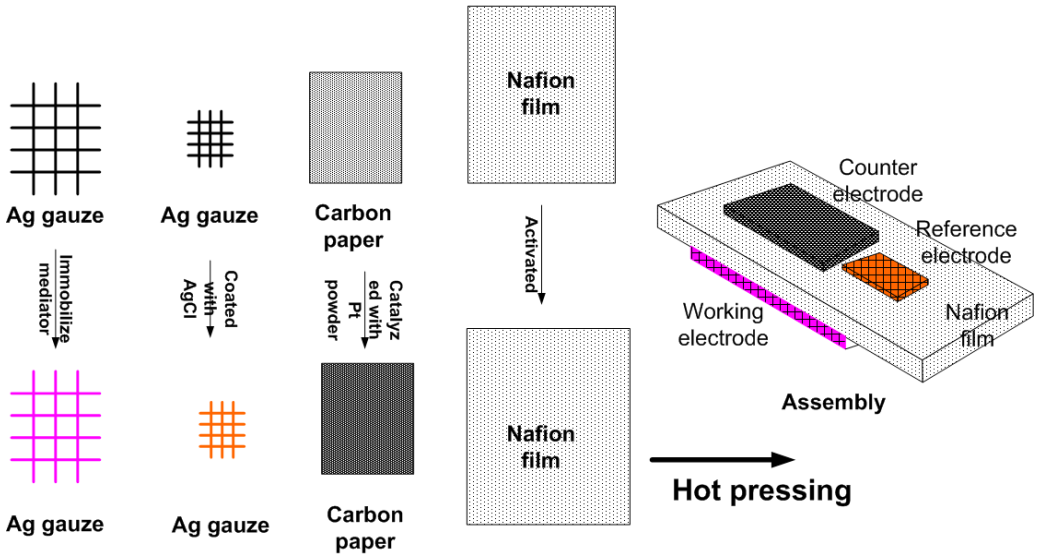

Figure 19 Procedure of fabricating a solid-state electrochemical sensor

3.2 Samples

Plastic coupon samples

Acrylic plastic samples were made with a size of 4 cm x 4 cm. The surfaces of the samples were treated differently as follows:

1) Original surface (ORI sample).
2) Polished surface (POL sample). The sample surface was polished using a polishing paper (# 600).
3) Sulfuric acid treated surface (SUL sample). The sample was dipped into 50% sulfuric acid for 2-5 seconds, withdrawn, rinsed and dried. This surface is supposed to have been deeply oxidized.

Peel ply prepared coupon samples

Peel ply is defined as: a removable outside fabric ply molded onto the surface of a laminate to provide a chemically clean surface for bonding when it is removed.

Samples were cut from a piece of laminates covered with peel plies into coupons of 4 cm x 4 cm. The peel plies were peeled off from the laminates using a sharp knife. Surfaces of the samples were treated differently as follows:

1. Original surface (ORI sample).
2. Polished surface (POL sample). The surfaces were polished using a polishing paper (# 600).
3. Sulfuric acid treated surface (SUL sample). The samples are dipped into 50% sulfuric acid for 2-5 seconds, withdrawn, rinsed, and dried. This surface is supposed to have been deeply oxidized.

Experimental setup

The experimental setup is very simple. The sensor assembly is set on the surface of a sample with the working electrode ($AgNO_3$ coated Ag gauze) in contact with the surface of the sample. A weight of 1 about one kg is placed on the top of the sensor assembly as shown the Figure 20. The electrodes are connected with a Gmery electrochemical measurement system (Gmery Instrument Inc.). Cyclic voltammetry measurements were conducted. The scanning speed was 50 mV/min for total five cycles. The scanning range was from -0.7 V to 0.7 V.

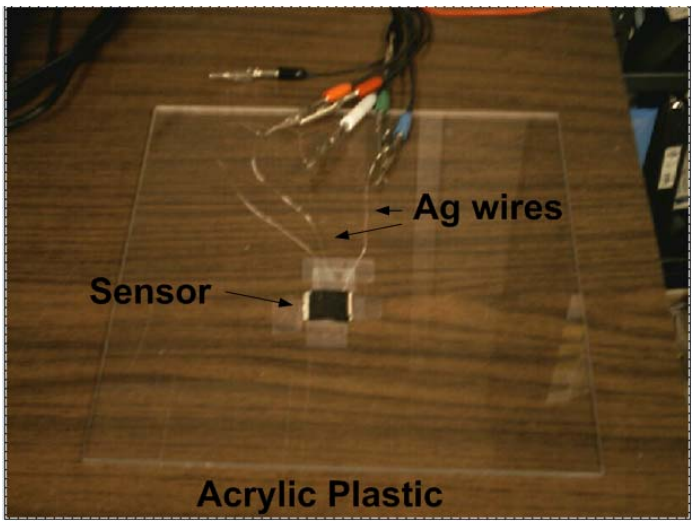

Figure 20 Experimental setup for surface electrochemical analysis on a piece of acrylic plastic

CHAPTER 4 Results

In order to evaluate the noise level of the sensor, a sensor was hung in air and the cyclic voltammetry measurement was conducted. The results are shown in Figure 21. The current level is very low (<10^{-4} A). Any current level greater than this baseline current can be considered as a meaningful signal from the interaction between the working electrode and the sample surface. The experimental results are illustrated in Figures 22, 23, and 24.

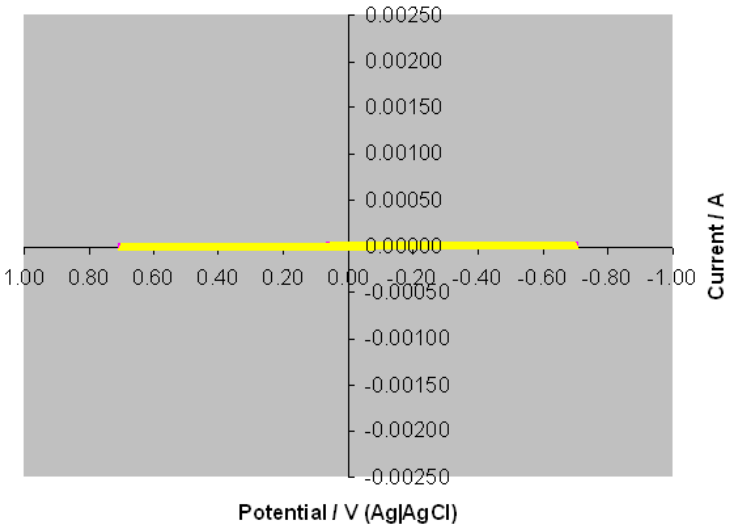

Figure 21 The cyclic voltammetry curves when the sensor was hung in air without contact with a sample surface

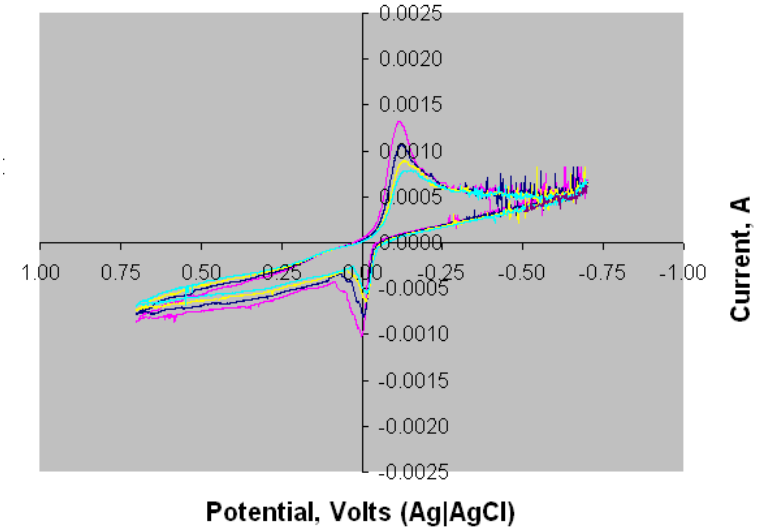

Figure 22 Cyclic voltammetry for the specimen with an original surface of an acrylic plastic sample

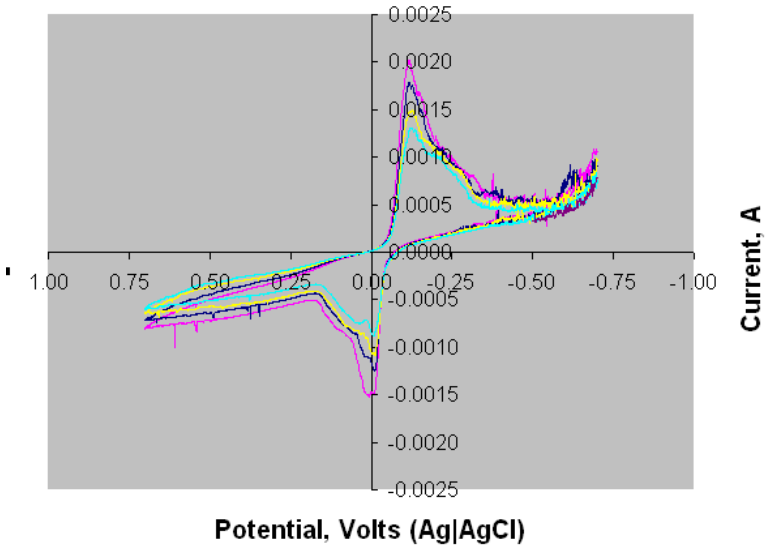

Figure 23 Cyclic voltammetry for the specimen with a polished surface of an acrylic plastic sample

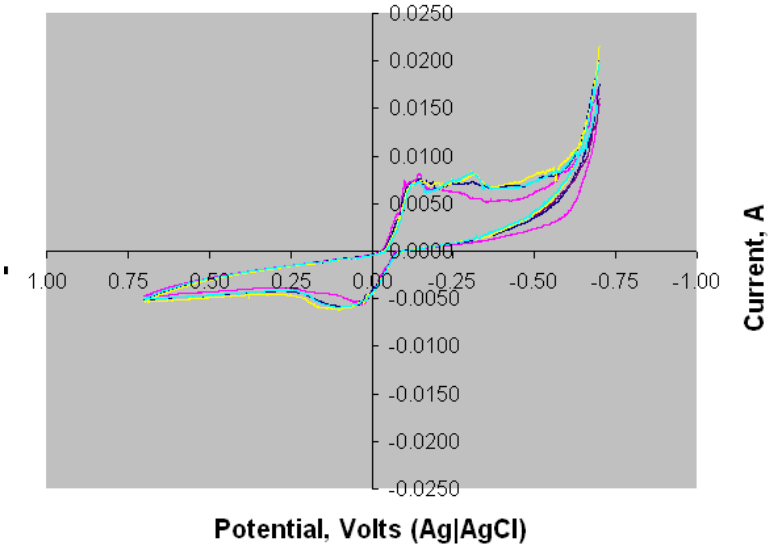

Figure 24 Cyclic voltammetry for the specimen with a surface of an acrylic plastic sample treated with sulfuric acid

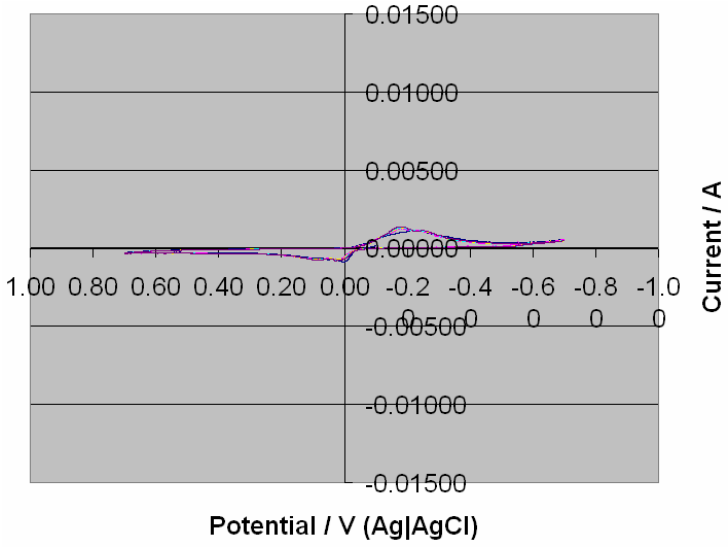

Figure 25 Cyclic voltammetry for the specimen with an original surface of composite laminate surface prepared with peel ply

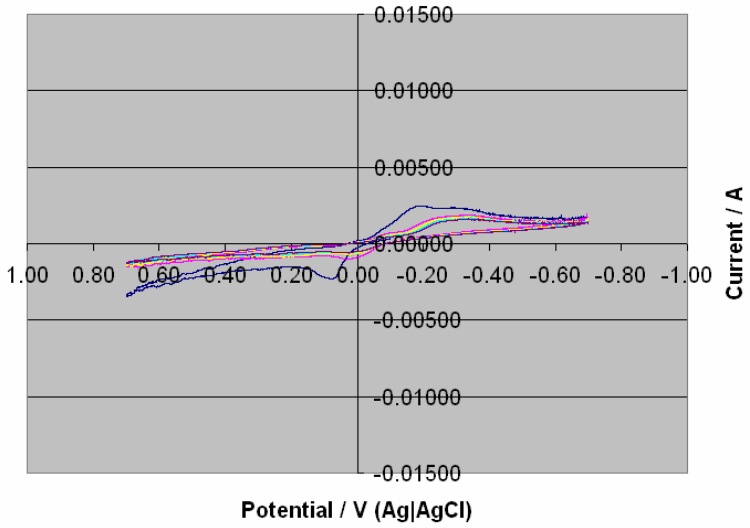

Figure 26 Cyclic voltammetry for the specimen with an original surface of composite laminate surface that was prepared with peel ply and polished

The electric current level for the sample treated in sulfuric acid is one order of magnitude greater that those for the original and polished samples. These results demonstrate that the sensor can tell the chemical differences between clean and slightly contaminated surfaces. Similar results were obtained for composite laminate surfaces prepared with peel plies as shown in Figures 25, 26 and 27.

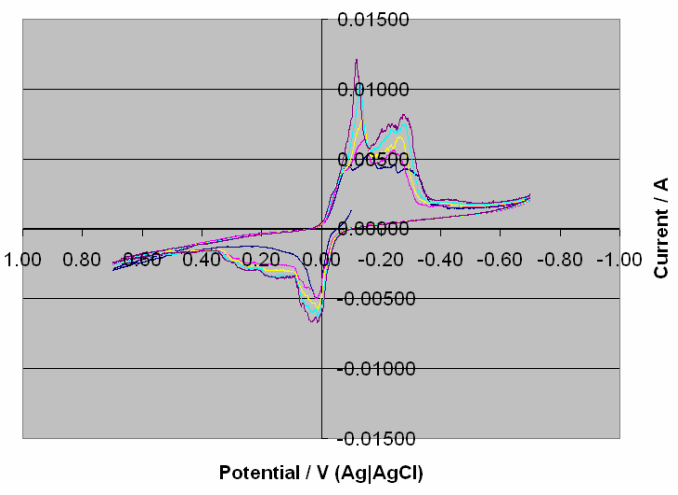

Figure 27 Cyclic voltammetry for the specimen with an original surface of composite laminate surface that was prepared with peel ply and treated with 50% sulfuric acid

In addition to Ag(I)/Ag(II) mediator, Mn(II)/Mn(III), Ce(III)/Ce(IV), and Cu(I)/Cu(II) were also be used to fabricate the electrochemical sensors using similar approaches. The results are presented in Figs. 28-30.

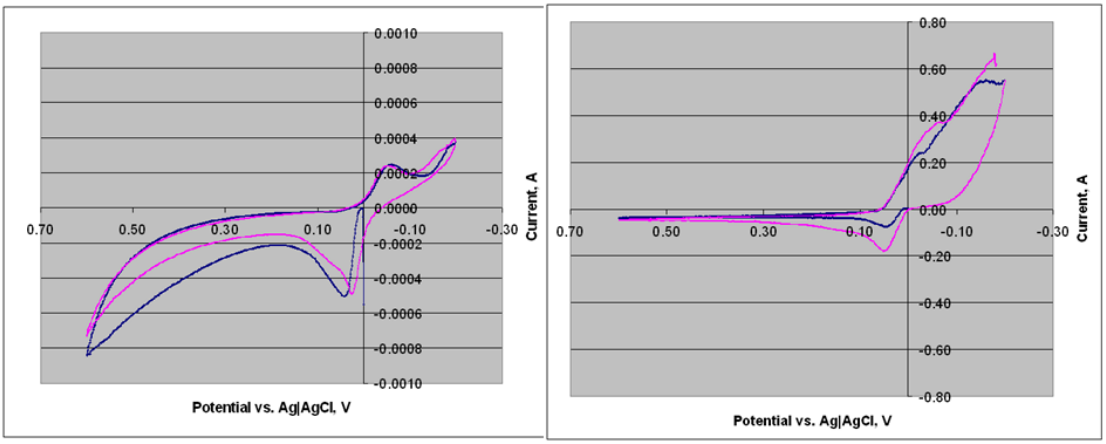

Figure 28 Cyclic voltammetry curves obtained using Mn(II)/Mn(III) mediators. Left: on original peel ply prepared sample. Right: on sulfuric acid contaminated sample

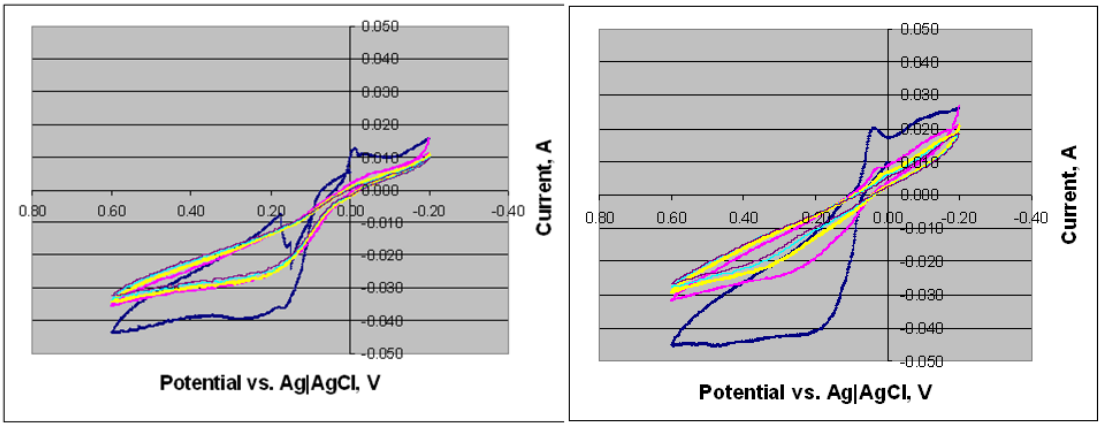

Figure 29 Cyclic voltammetry curves obtained using Ce(III)/Ce(IV) mediators. Left: on original peel ply prepared sample. Right: on sulfuric acid contaminated sample.

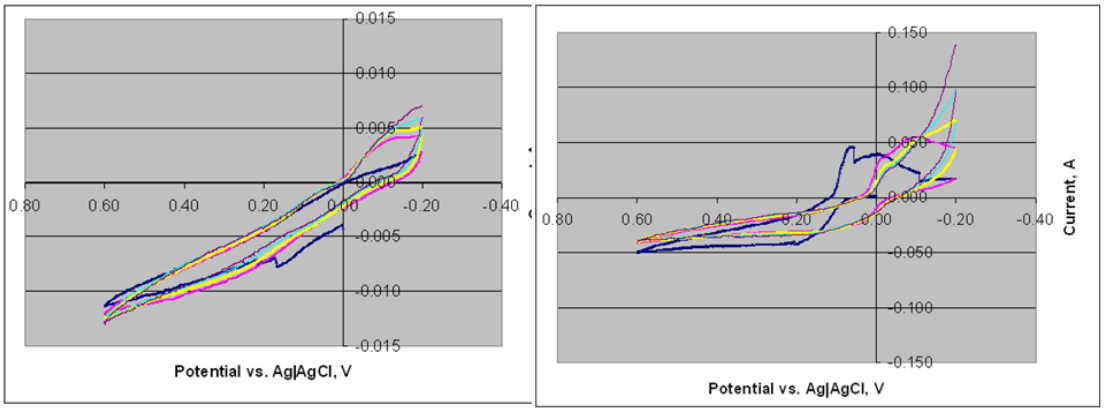

Figure 30 Cyclic voltammetry curves obtained using Cu(I)/Cu(II) mediators. Left: on original peel ply prepared sample. Right: on sulfuric acid contaminated sample.

If the fresh peel ply prepared samples are considered as having low contamination level or as being uncontaminated and those treated with sulfuric acid are considered as contaminated samples, the sensitivity of the solid-state electrochemical sensors can be evaluated using the ratio of the maximum current for uncontaminated sample to that for contaminated sample. The sensitivity evaluations are listed in Table 6. It is clear that Mn(II)/Mn(III), Cu(I)/Cu(II) and Ag(I)/Ag(II) mediators result in significant sensitivity of the contamination.

Table 6 Maximum cathodic currents and maximum anodic currents for pristine (original) samples and sulfuric acid contaminated samples and their ratios.

Mediator	I_{ca} (ori)	I_{an} (ori)	I_{ca} (sul)	I_{an} (sul)	I_{ca} (sul)/ I_{ca} (ori)	I_{an} (sul)/ I_{an} (ori)
Ag(I)/Ag(II)	0.0048	0.0052	0.022	0.0048	4.58	0.923
Mn(III)/Mn(IV)	0.0004	0.00081	0.65	0.18	1625.0	222.2
Ce(III)/Ce(IV)	0.015	0.042	0.026	0.045	1.733	1.071
Cu(I)/Cu(II)	0.0055	0.0125	0.145	0.05	26.4	4.0

CHAPTER 5 Discussion

5.1Analysis of cyclic voltammetry

5.1.1 Reversible system

The potential is swept linearly at v (V/s) so that the potential at any time is

$$E(t) = E_i - vt \tag{12}$$

where E_i is the initial potential.

The current-time curve or, since potential is linearly related to time, the current-potential equation is given below:

$$i = nFAC_O^*(\pi D_O \sigma)^{1/2}\chi(\sigma t) \tag{13}$$

Which is the solution of the equation [75]:

$$\int_0^{\sigma t} \frac{\chi(z)dz}{(\sigma t - z)^{1/2}} = \frac{1}{1+\xi\theta S(\sigma t)} \tag{14}$$

$$S(\sigma t) = e^{-\sigma^2 t} \tag{15}$$

$$\theta = \exp[\frac{nF}{RT}(E_i - E^{0'})] \tag{16}$$

$$\sigma = \frac{nF}{RT}v \tag{17}$$

$$\xi = \left(\frac{D_O}{D_R}\right)^{1/2} \tag{18}$$

Where C_O^* is the bulk concentration of O;

$\chi(z)$ is the normalized current for a reversible system in LSV and CV;

n is stoichiometric number of electrons involved in an electrode reaction;

A is the area of the electrode;

F is the Faraday constant, which is 96485;

R is the universal gas constant, which is 8.31;

T is temperature, here is 298K;

E_i is the initial potential;

$E^{0'}$ is the formal potential;

v is the scan rate;

D_O and D_R are the diffusion coefficient of oxidation and reduction species, respectively.

The numerical solution by Nicholson and Shain [76] as a function of ct or $n(E - E_{1/2})$ are shown in the Table 7. Fig. 31 shows a complete cycle of cyclic voltammetry according to the solution.

Table 7 Current Functions for Reversible Charge Transfer

$n(E - E_{1/2})$ mV at 298K	$\pi^{1/2}\chi(\sigma t)$	$n(E - E_{1/2})$ mV at 298K	$\pi^{1/2}\chi(\sigma t)$	$n(E - E_{1/2})$ mV at 298K	$\pi^{1/2}\chi(\sigma t)$
120	0.009	20	0.269	-80	0.353
110	0.013	10	0.328	-90	0.33
100	0.02	0	0.38	-100	0.312
90	0.029	-10	0.418	-110	0.294
80	0.042	-20	0.441	-120	0.28
70	0.06	-30	0.449	-130	0.268
60	0.084	-40	0.438	-140	0.255
50	0.117	-50	0.421	-150	0.245
40	0.16	-60	0.399		
30	0.211	-70	0.375		

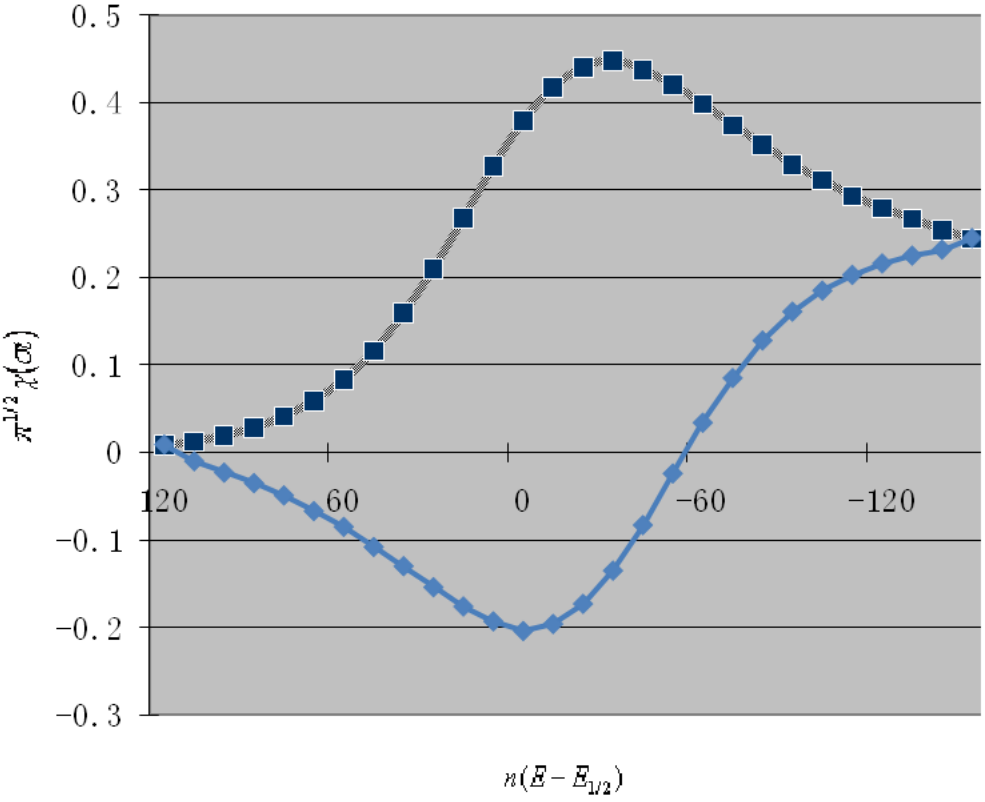

Figure 31 Linear potential sweep voltammogram in terms of dimensionless current function for reversible systems. Values on the potential axis are for 298 K

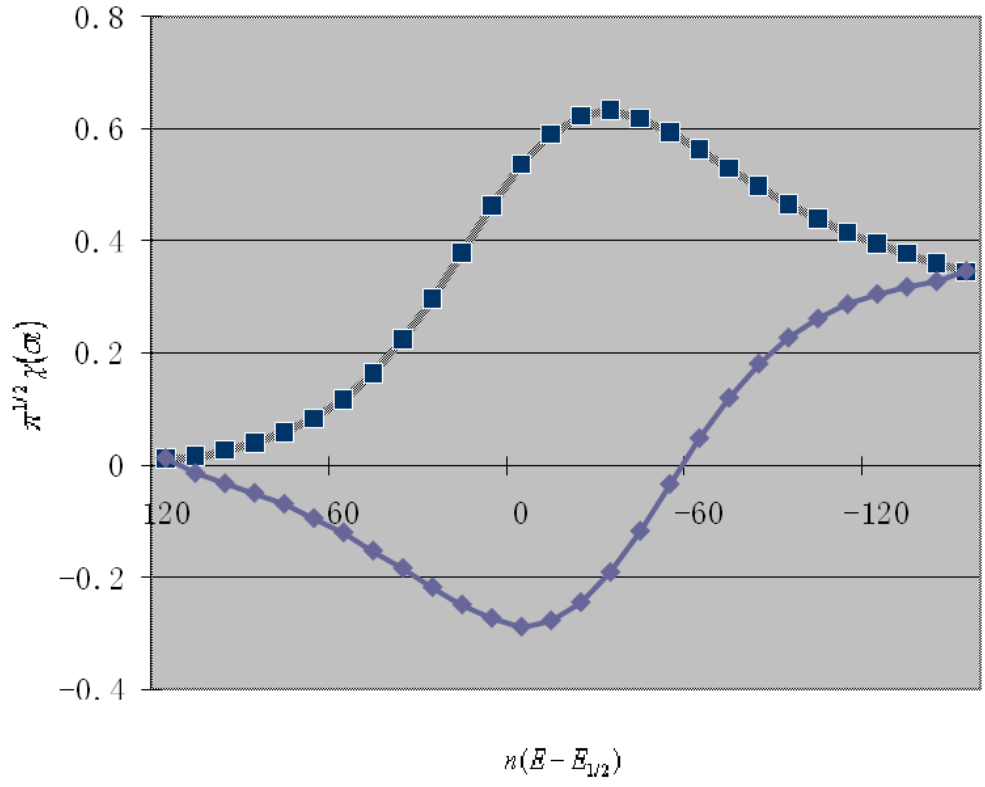

Figure 32 The curves when the scan rate is doubled. The current i amplified by the factor of $\sqrt{2}$.

5.1.2 Quasi-reversible system

In a quasi-reversible system, the current function is given by:

$$i = FAD_O^{1/2} C_O^* f^{1/2} v^{1/2} \Psi(E) \tag{19}$$

where $\Psi(E)$ is shown in Fig. 33, define

$$\Lambda = \frac{k^0}{(D_O^{1-\alpha} D_R^{\alpha} fv)^{1/2}} \tag{20}$$

as the equivalent conductivity of solution, where

k^0 is the standard heterogeneous rate constant,

$$f = \frac{F}{RT} \tag{21}$$

α is the transfer coeffient

When Λ>10, the behavior approaches that of a reversible system. For a quasi-reversible reaction, the peak current i_p is not proportional to $v^{1/2}$

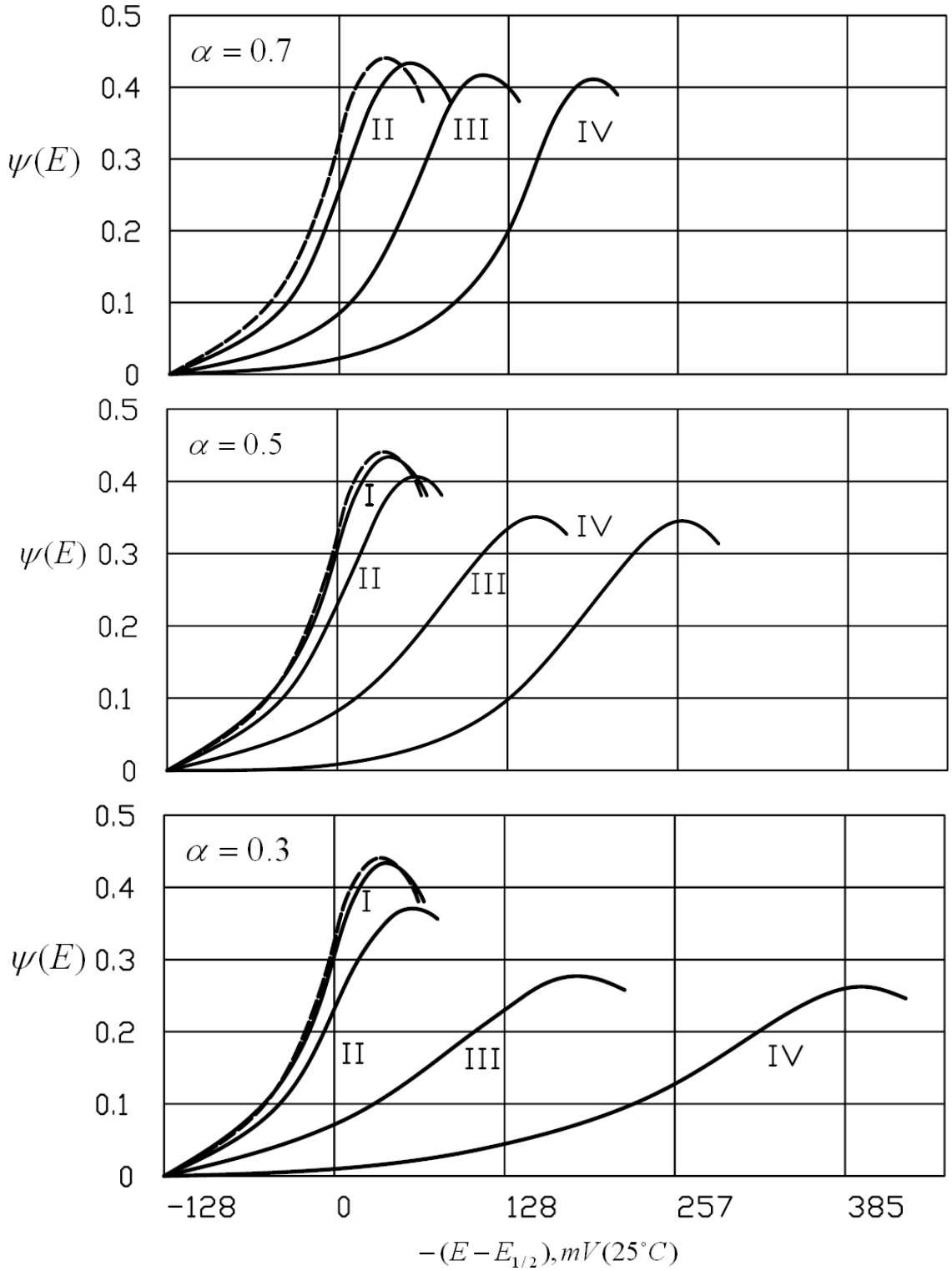

Figure 33 variation of quasi-reversible current function, $\Psi(E)$, for different α and Λ

(I) Λ=10; (II) Λ=1; (III) Λ= 0.1; (IV) Λ=0.01, dashed curve is for a reversible reaction.

For $D_O = D_R = D$,

$$\Psi(E) = \frac{i}{FAC_O^* D_O^{1/2} \left(\frac{nF}{RT}\right)^{1/2} v^{1/2}} \tag{22}$$

And $$\Lambda = \frac{k^0}{D^{1/2} \left(\frac{F}{RT}\right)^{1/2} v^{1/2}} \tag{23}$$

We can see that with the decrease of the magnitude of Λ, the system is more irreversible, the voltammogram getting extend.

Typical i-t curves for different switching potentials are shown in Fig. 34.

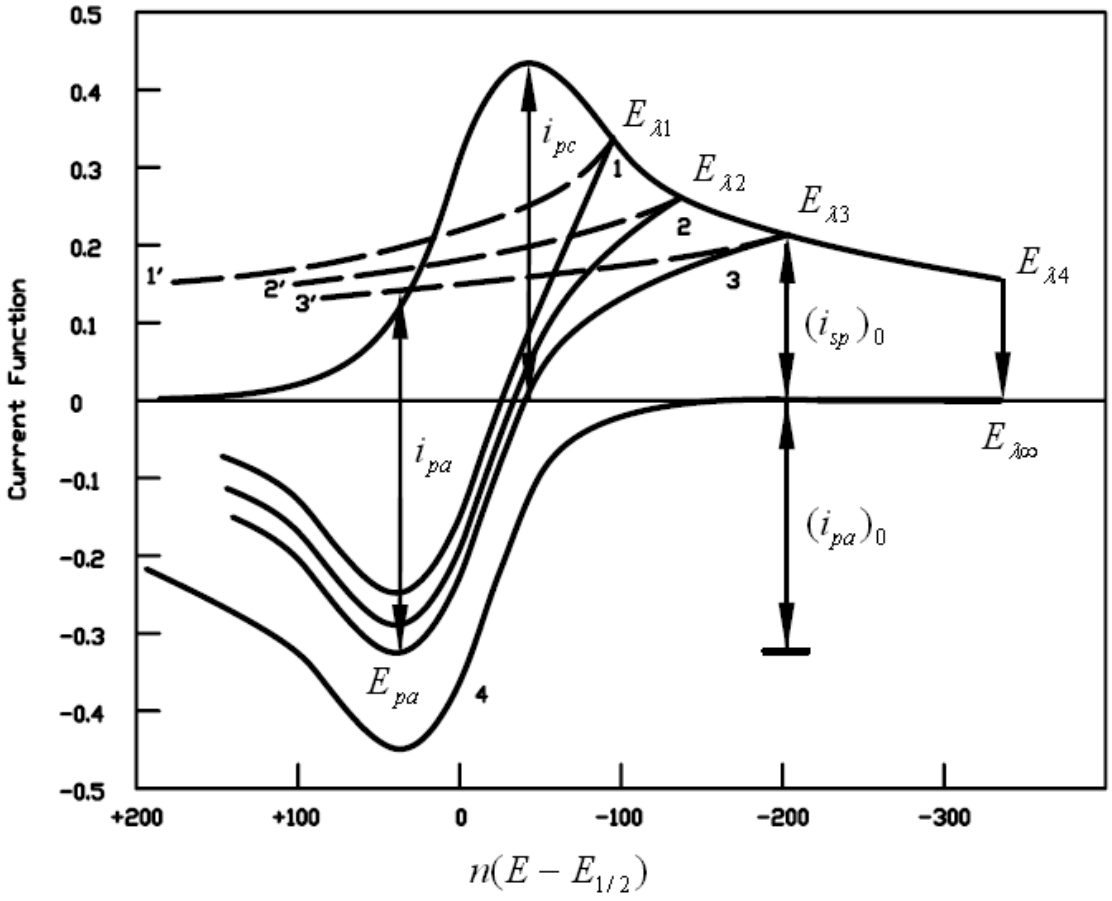

Figure 34 Cyclic voltammograms for reversible at different E_λ values, with presentation on a time base

Use the current peak equation to calculate the diffusion coefficient D_0:

$$i_p = (2.69\times10^5)n^{3/2}AD_O^{1/2}C_0^*v^{1/2} \quad (24)$$

n=1, A=1cm^2, C_0^*=0.5, v=50, deriving:

$$D_O = \frac{i_p^2}{9\times10^5} \quad (25)$$

Table 8 The peak potential and current values of both peaks of each Figure

Sample	Peak width ΔE_w(V)	$E_{p,c}$(V)	$I_{p,c}$(mA)	$E_{p,a}$(V)	$I_{p,a}$(mA)	ΔE_p(V)	D_0
Hang in air	--	--	0	--	0	--	--
Original	0.08	-0.12	1.3	0	-1.0	0.12	1.88×10^{-6}
Polished	0.13	-0.12	2.0	0	-1.5	0.12	4.44×10^{-6}
Sulfuric acid washed	0.20	-0.15	8.3	0.03	-5.0	0.18	7.65×10^{-5}
Peel ply (original)	0.23	-0.18	1.5	0	-0.8	0.18	2.50×10^{-6}
Peel ply polished	0.32	-0.19	2.4	0.08	-2.1	0.29	6.40×10^{-6}
Peel ply acid washed main peak	0.29	-0.12	12.1	0.02	-6.7	0.14	1.63×10^{-4}

5.2 Epoxy surface oxidized by sulfuric acid

There are three molecular groups generated from the reactions between epoxy and sulfuric acid [77]: ketone group, hydroxyl group and carboxic acid group. The reactions are shown below:

1) **Ketone**

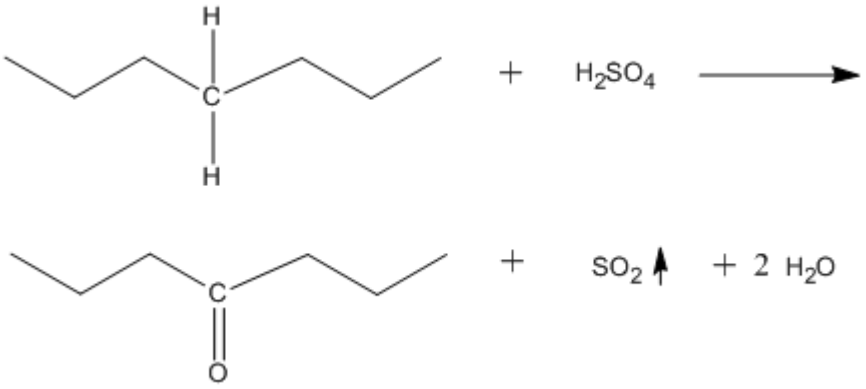

Figure 35 The reaction that generates ketone

2) **Hydroxyl**

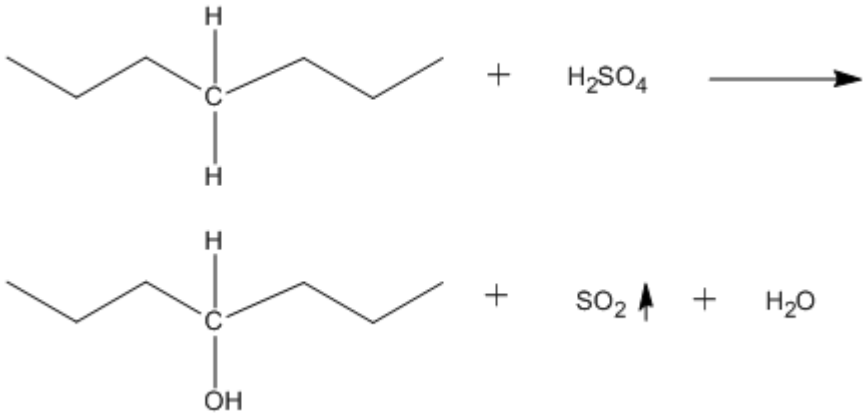

Figure 36 The reaction that generates hydroxyl

5.3 Electrochemical reactions at sensor and epoxy interface (in the anodic half cycle of cyclic voltammetry)

When the surface is in contact with attached by the sensor, the silver ion will oxidize the surface resulting in an anodic current.

Surface oxidized

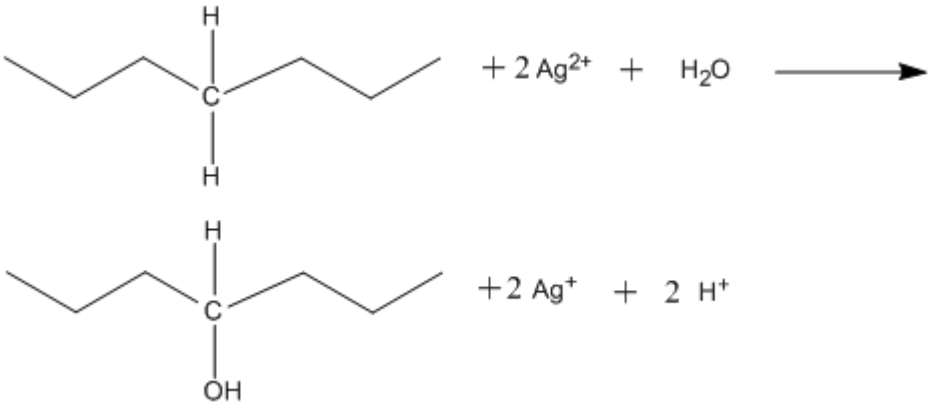

Figure 37 polymer surface oxidized by silver ion

5.4 Electrochemical reactions at sensor and epoxy interface (in the cathodic half cycle of cyclic voltammetry)

The group oxidized by the sulfuric acid will be reduced by the Ag^{+} ion. The reactions are shown below:

1) Ketone

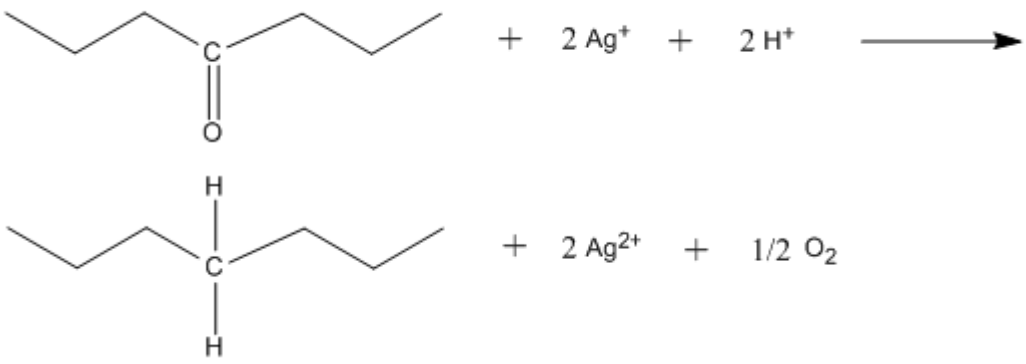

Figure 38 Ketone group reduced by silver ion

2) Hydroxyl

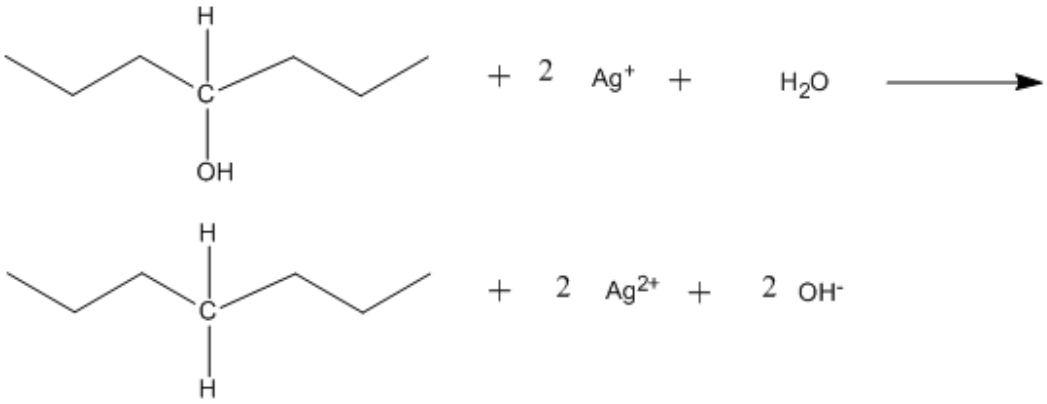

Figure 39 Hydroxyl group reduced by silver ion

3) Epoxy

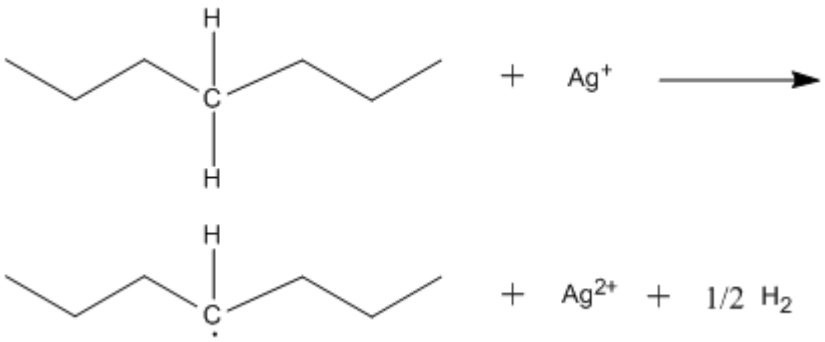

Figure 40 Epoxy structure reduced by silver ion

5.5 Theoretical analysis

According to Table 8 and the mechanism above, the author would make some observations as below:

1) When the sample is hung in the air, the current value is insignificant ($<10^{-4}$ A). By setting this as a reference, any current value significantly greater than this reference value could be an indication of interaction between the sample surface and the sensor.

Regarding the original acrylic polymer sample (Figure 22), the reduction peak is above the X axis while the oxidation peak is below the X axis. The magnitude of the reduction peak is greater than that of the oxidation peak. According to Table 8,

$$\frac{\left|I_{p,c} - I_{p,a}\right|}{I_{p,a}} \times 100\% = 30\% \tag{26}$$

which indicates that the system is asymmetric. Actually for all the other samples listed in Table 8 the cyclic voltammetry curves show similar asymmetry. The reason is probably because some of the reactions happened on the surface are not reversible such as those in Figs 38-41.

2) The surface energy of the polished surface is increased. The current values for polished samples especially the peak current value is increasedin comparison to the values for original samples. The current and the activation energy has the relation:

$$I = A\exp\left(\frac{-\Delta E_{act}}{RT}\right) \tag{27}$$

The polishing process increases the activation energy so the overall current figure moves upward as shown in Fig. 41 .

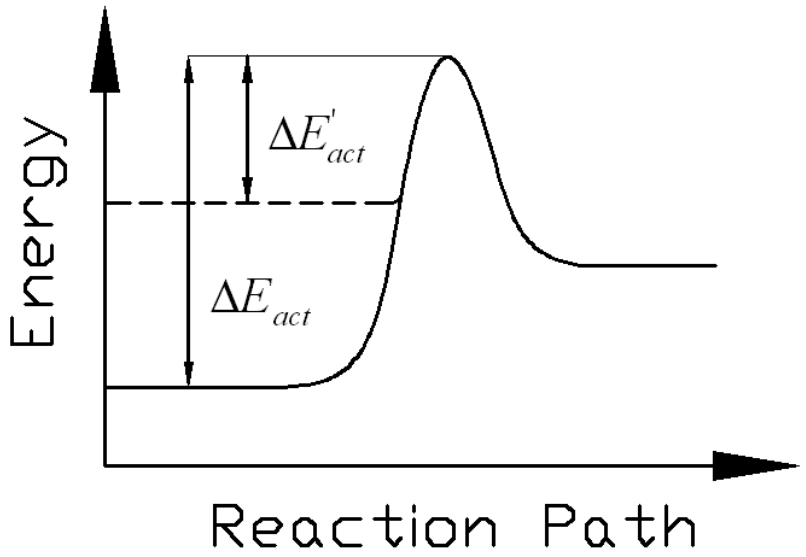

Figure 41 Activation energy of the reaction versus reaction path

3) From Table 8, ΔE_p for all the samples are 120, 180, 290 and 140 mV. However, for any reversible electrochemical reaction,

$$\Delta E_p = 59/n \text{ (mV)} \quad (28)$$

where n is the number of electrons involved in the reactions. The greater ΔE_p values obtained the experiment indicate that the reactions on the surface are irreversible according to the analysis of cyclic voltammetry for irreversible systems shown in Fig. 33.

4) The width of the reduction peak (at half height) for both sulfuric acid washed samples are broadened in comparison to the original samples. In the case of arylic polymer the increase was 250% while for peel ply prepared sample the increase was 126%. The reason may be that the treatment by sulfuric acid generated a lot of oxidized molecules and functional groups as being explained in Section 5.2.3.

5) The peak current, I_p for both sulfuric acid washed samples are much larger than other samples as shown in Table 8.This suggests that redox reactions occur on these sulfuric acid treated surfaces more extensively because on these

surfaces there are contaminations in the forms of oxidized molecules, molecular clusters, and functional groups.

6) With respect to diffusivity of mediator evaluated using Equation 25 shown in Table 8, there are several observations and explanations as follows.

The diffusivity of silver ions in the presence of Ag^{+} and Ag^{2+} is given by [78] which is:

$$D_{AX}' = D_{AX} + \frac{k\delta_{AX}{}^{2}\pi}{4} c_A \tag{29}$$

where D_{AX} is the original diffusivity, D_{AX}' is the diffusivity with the +2 silver ion, k is constant, δ_{AX} is the distance between the +1 silver ion and the +2 silver ion. c_A is the concentration. Thus, essentially, the diffusivity of Ag^{+} in the presence of Ag^{2+} should be greater than that when there is no Ag^{2+}. We could see that the diffusivity of the ion on the original sample was one order of magnitude smaller than the Ag ion diffusivity (without Ag^{2+}) in the water, 1.3×10^{-5} cm^2 s^{-1} [79]. It is commonly accepted that the mobility of Ag ions in solid state electrolyte is lower than that in liquid electrolyte. Thus, the first term in Eq. (29) dominates.

On the the sulfuric acid treated samples, the diffusivity is at least 40 times greater than that on the original sample and 5 times greater than Ag ion diffusivity in water, 1.3×10^{-5} cm^2 s^{-1}. The author suggests two possible reasons for the observed high diffusivity. The first is that the surface is greatly oxidized resulting in small molecules such as water and fragments of polymer thereby leading to the better mobility of the Ag(I) and Ag(II) ion. The second is that sulfuric acid oxidizing process generates some other substance on the surface which than get involved in the redox reaction at a higher reaction rate.

CHAPTER 6 Conclusion

In this study, adhesive bonding, surface pretreatment, non-destructive inspection methods have been reviewed. A new solid-state electrochemical sensor for adherend surface property evaluation has been developed. Two kinds of materials are tested: acylic plastics and peel ply prepared composite material. In addition to original or pristine sample surfaces, polishing and sulfuric acid washed surfaces were also used to demonstrate the sensitivity of the sensor to surface contamination. The conclusions are stated below:

1) In aviation industry quality assurance for pre-bonding surface preparations relies on tedious and tight control of the processes. This may result in excess or inadequate treatment that may cause high costs or weak bonds.
2) A definitive, online, and in-field method for surface chemistry analysis is required to improve the aircraft manufacture processes.
3) An all solid-state electrochemical sensor is developed and is demonstrated to be able to indicate contamination substance on the surface with a high sensitivity. In other words, through analyzing the output cyclic voltammogram, the sample's surface contamination level and chemical condition can be determined.
4) The Ag(I)/Ag(II), Cu(I)/Cu(II), and Mn(II)/Mn(III) ions as redox pairs are effective in detecting surface contanmination level.
5) Sulfuric acid treatments produce small molecules and polymer fragments and introduce water. These contaminants tend to be reduced but are less likely to be oxidized. Thus most of the electrochemical reactions are irreversible.
6) Polishing treatment will increase the surface energy and reduce the

activation energy resulting in increase of the peak current of the output cyclic voltammogram.

References

[1] Navy Joining Center, NJC Completes Adhesive Bonding Project for Primary Aircraft Structures.

[2] Identification: DCA88MA054, NTSB, Maui, HI, April 28, 1988.

[3] Investigation report 3X164-0/03, German Federal Bureau of Aircraft Accidents Investigation. April 2006.

[4] Report No. 1/2006 (EW/C2004/07/06), Air Accidents Investigation Branch, Department of Transport.

[5] A. Baldan, "Review adhesively-bonded joints and repairs in metallic alloys, polymers and composite materials: adhesives, adhesion theories and surface pretreatment," J. Material Science 39(2004), 1-49.

[6] K. W. Allen, "'At forty cometh understanding' a review of some basics of adhesion over the past four decades," Int. J. Adhes. & Adhes. 23(2003), 87-93.

[7] R. D. Adams, Adhesive Bonding. Woodhead Publishing Limited, Cambridge, GBR, 2005.

[8] G. A. Jeffrey, An Introduction to Hydrogen Bonding, Oxford University Press. New York, 1997.

[9] R. S. Drago, G. C. Vogel and T. E. Needham, "Four-parameter equation for predicting enthalpies of adduct formation," J. Amer. Chem. Soc 93(1971), 6014-6026.

[10] M. Davis and D. Bond, "Principles and practices of adhesive bonded structural joints and repairs," Int. J. Adhes. & Adhes. 19(1999), 91-105.

[11] N. E. Dowling, Mechanical behavior of materials: engineering methods for deformation, fracture and fatigue, Upper Saddle River, NJ, Prentice Hall, 1998.

[12] S. H. Myhre, J. D. Labor and S. C. Aker, "Moisture problems in advanced composite structural repair," Composites 13(1982), 289-297.

[13] J. Comyn, Durability of Structural Adhesives, A. J. Kinloch ed., Applied Science Publishers, London, Ch 3, p. 85. 1983.

[14] A. J. Kinloch, Durability of Structural Adhesives, A. J. Kinloch ed., Applied Science Publishers, London, Ch 1, p 1, 1983.

[15] R. A. Flinn and P. K. Trojan, Engineering Materials and Their Applications, 4th ed., John and Wiley Sons, Inc., p.608,1995.

[16] P. Molitor, V. Barron and T. Young, "Surface treatment of titanium for adhesive bonding to polymer composites: a review," Int. J. Adhes. & Adhes. 21(2001), 129-136.

[17] J. Wingfield, “Treatment of composite surfaces for adhesive bonding,” Int. J. Adhes. & Adhes. 13(1993), 151-156.

[18] A. J. Kinloch, Adhesion and adhesives: Science and Technology, Chapman & Hall, London, p. 123-127, 1987.

[19] J. Comyn, L. Mascia and G. Xiao, “Corona-discharge treatment of polyetheretherketone(PEEK) for adhesive bonding,” Int. J. Adhes. & Adhes. 16(1996), 301-304.

[20] Q. Benard, M. Fois and M, Grisel, “Influence of fibre reinforcement and peel ply surface treatment towards adhesion of composite surfaces,” Int. J. Adhes. & Adhes. 25(2005), 404-409.

[21] M. Noeske, J. Degenhardt, S. Strudthoff and U.Lommatzsch, “Plasma jet treatment of five polymers at atmospheric pressure: surface modifications and the relevance for adhesion,” Int. J. Adhes. & Adhes. 24(2004), 171-177.

[22] A. F. Harris and A. Beevers, “The effects of grit-blasting on surface properties for adhesion,” Int. J. Adhes. & Adhes. 19(1999), 445-452.

[23] M. H. Stone, “Effect of degree of abrasion of composite surfaces on strengths of adhesively bonded joints,” Int. J. Adhes. & Adhes. 1(1981), 271-272.

[24] A. Bjorgum, F. Lapique, J. Walmsley and K. Redford, “Anodising as pre-treatment for structural bonding,” Int. J. Adhes. & Adhes. 23(2003), 401-412.

[25] P. H. Winfield, A. F. Harris and A. R. Hutchinson, “The use of flame ionisation technology to improve the wettability and adhesion properties of wood,” Int. J. Adhes. & Adhes. 21(2001), 107-114.

[26] Q. Bénard, M. Fois, M. Grisel and P. Laurens, “Surface treatment of carbon/epoxy and glass/epoxy composites with an excimer laser beam,” Int. J. of Adhes & Adhes. 26(2006), 543-549.

[27] C. L. Olson-Jacques, A. R. Wilson, A. N. RIDER and D. R. Arnott, Surf. Interface Anal. 24(1996), 569.

[28] A. N. Rider and D. R. Arnott, Surf. Interface Anal. 24(1996), 583.

[29] S.L. Rosen, Fundamental Principles of Polymeric Materials, 2nd ed. John Wiley and Sons, 1993.

[30] M. Michaloudaki, E. Lehmann and D. Kosteas, “Neutron imaging as a tool for the non-destructive evaluation of adhesive joints in aluminum,” Int. J. Adhes. & Adhes. 25(2005), 257-267.

[31] C. J. Hellier, Handbook of Non-destructive Evaluation, McGraw-Hill, 2001.

[32] S. K. Tomlinson, O. R. Ghita, R. M. Hooper and K.E. Evans, "The use of near infrared spectroscopy for the cure monitoring of adhesives," Vibrational Spectroscopy 40(2006), 133-141.

[33] C. Bockenheimer, D. Fata, W. Possart, M. Rothenfusser, U. Netzelmann and H. Schaefer, "The method of non-linear ultrasound as a tool for the non-destructive inspection of structural epoxy-metal bonds – a résumé," Int. J. Adhes. & Adhes. 22(2002), 227-233.

[34] M. Genest, M. Martinez, N. Mrad, G. Renaud and A. Fahr, "Pulsed thermography for non-destructive evaluation and damage growth monitoring of bonded repairs," Composite Structures (2008), doi: 10.1016/j.compstruct.2008.02.010.

[35] H. Nayeb-Hashemi, D. Swet and A. Vaziri, "New electrical potential method for measuring crack growth in nonconductive materials," Measurement 36(2004), 121-129.

[36] J. R. Scully, "Electrochemical Impedance of Organic-Coated Steel: Correlation of Impedance Parameters with Long-Term Coating Deterioration," J. Electrochem. Soc. 136(1989), 979-990.

[37] L. J. Hart-Smith, "A peel-type durability test coupon to assess interface in bonded, co-bonded, and co-cured composite structure," Int. J. Adhes. & Adhes. 19(1999), 181-191.

[38] J. W. Chin and J. P. Wightman, "Surface characterization and adhesive bonding of toughened bismaleimide composite," Composites 27A(1996), 419-428.

[39] J. Bardis, and K. Kedward, "Effect of surface preparation on the long-term durability of adhesive bonded composite structures," Technical Report, DOT/FAA/AR-03/53, January 2004.

[40] R. D. Adams and B.W. Drinkwater, "Nondestructive testing of adhesively-bonded joints," NDT&E International 30-2(1997), 93-98.

[41] K. B. Armstrong, "Effect of absorbed water in CFRP composites on adhesive bonding," Int. J. Adhes. & Adhes. 16(1996), 21-28.

[42] L. J. Hart-Smith, "Adhesive Bonding of Composite Structures-Progress Date and Some Remaining Challenges," (2002).

[43] FAA, to be available in the FAA website: http://www.niar.wichita.edu/faa, 2004.

[44] A. Higgins, "Adhesive bonding of aircraft structures," Int. J. Adhes. & Adhes. 20(2000), 267-276.

[45] M. J. Davis, "A call for minimum standards in design and application technology for bonded structure repairs. Proc. Symp on Composite Repair of Aircraft Structures," Vancouver, 4-15, (1995).

[46] A. W. Espie, J.H. Rogerson, and K. Ebtehaj, "Quality assurance in adhesive technology," Int. J. Adhes. & Adhes. 15(1995), 81-85.

[47] W. S. Johnson, L.M. Butkus, and R.V. Valentin, "Application of fracture mechanics to the Durability of bonded composite joints," Final Report: DOT/FAA/AR-97/56, 1998.

[48] D. L. Woerdeman, J.A. Emerson, and R.K. Giunta, :JKR contact mechanics for evaluating surface contamination on inorganic substrates," Int. J. Adhes. & Adhes. 22(2002), 257-264.

[49] W. Wang, and A.V. Virkar, "A conductimetric humidity sensor based on proton conducting perovskite oxides," Sensors and Actuators B98(2004), 282-290.

[50] P. M. Faia, C.S. Furtado, and A. J. Fereirra, "Humidity sensing properties of a thick-film titiania prepared by slow spinning process" Sensors and Actuators B101(2004), 183-190.

[51] G. D. Davis and L. A. Krebs, "Electrochemical sensors for nondestructive evaluation of adhesive bonds," Final Report, #A810173, DACCO SCI Inc., Oct. 1999.

[52] G. D. Davis, C.M. Dacres, and L. A. Krebs, http://www.corrosion-doctors.org/Journal-2000/No1/TitleNo1.htm.

[53] J. Wang, N. Foster, S. Armalis, D. Larson, A. Zirino, and K. Olsen, "Remote stripping electrode for in situ monitoring of labile copper in marine environment," Analytica Chimica Acta 310(1995), 223-231.

[54] J. P. Coleman and D. Pletcher, "Some comments on the mechanism of the oxidation of alkanes at a Pt anode in fluorosulphonic acid," J. Electroanal. Chem. 87(1978), 111-117.

[55] L. Eberson, J. H. P. Utley and O. Hammerich, In: H. Lund and M. M. Baizer, editors. Organic Electrochemistry. 3rd ed. New York: Marcel Dekker, P. 514. 1991.

[56] M. Fleischmann, D. Pletcher and A. Rafinski, "The kinetics of the silver (I)/silver (II) couple at a platinum electrode in perchloric and nitric acids," J. Appl. Electrochem. 1(1971), 1-7.

[57] J. Bringmann, K. Ebert, U. Galla and H. Schmieder, "Electrochemical mediators for total oxidation of chlorinated hydrocarbons: formation kinetics of Ag(II), Co(III), and Ce(IV)," J. Appl. Electrochem. 25(1995), 846-851.

[58] K. B. Wiberg and R. Eisenthal, "On the mechanism of the oxidation of hydrocarbons with chromic acid and chromyl chloride," Tetrahedron 20(1964), 1151-1161.

[59] J. C. Farmer, F. T. Wang, R. A. Hawley-Fedder, P. R. Lewis, L. J. Summers and L. Foiles, ”Electrochemical treatment of mixed and hazardous wastes: oxidation of ethylene glycol and benzene by silver (II).,” J. Electrochem. Soc. 139(1992), 654-662.

[60] A. Paire, D. Espinoux, H. Masson and H. Lecomte, “Silver(II) mediated electrochemical treatment of selected organics: hydrocarbon destruction mechanism,” Radiochim. Acta 78(1997), 137-143.

[61] D. M. Brewid, R. H. Dahm and I. Mathieson, “Electrochemical pretreatment of polymers with dilute nitric acid either alone or in the presence of silver ions,” J. Adhes. 72 (2000), 373-386.

[62] G. O. Ybarra, C. A. Moina, M.I. Floritb and D. Posadas, “Redox mediation at electroactive polymer coated electrodes: Mechanistic diagnosis criteria from steady state polarization curves,” J. of Electroanal. Chem. 609(2007), 129-139.

[63] R. W. Murray (Ed.), Molecular Design of Electrode Surfaces, Wiley, New York, 1992.

[64] M. E. G. Lyons (Ed.), Electroactive Polymer Electrochemistry, Plenum Press, New York, 1996.

[65] E. Laviron, “A multilayer model for the study of space distributed redox modified electrodes: Part I. Description and discussion of the model,” J. Electroanal. Chem. 112(1980), 1–9.

[66] T. Ikeda, C. R. Leidner and R. W. Murray, “Kinetics of electron transfer reactions of metal complexes at impermeable redox active polymeric films on electrode surfaces and charge transport within the polymer film,” J. Electroanal. Chem. 138(1982), 343-365.

[67] F. C. Anson, J. -M. Saveant and K. Shigehara, “Self-exchange reactions at redox polymer electrodes: A kinetic model and theory for stationary voltammetric techniques,” J. Phys. Chem. 87(1983), 214-219.

[68] W. J. Albery and A. R. Hillman, ”Transport and kinetics in modified electrodes,” J. Electroanal. Chem. 170(1984), 27-49.

[69] P. Novak, K. Muller, K. S. V. Santhanam and O. Hass,” Electrochemically active polymers for rechargeable batteries,” Chem. Rev. 97(1997), 207-282.

[70] G. Ybarra, C. Moina, M. Ines Florit and D. Posadas, “Current rectification by mediating electroactive polymers,” Electrochim. Acta 53(2008), 3955-3959.

[71] V. Levich, Physicochemical Hydrodynamics, 2nd ed., Prentice Hall, Englewood Cliffs, NJ, 1962.

[72] K. A. Mauritz and R. B. Moore, “State of understanding of Nafion,” Chem. Rev. 104(2004), 4535-4585.

[73] Church, Steven. Del. firm installs fuel cell, The News Journal, p. B7, January 6, 2006.

[74] C. Heitner-Wirguin, "Recent advances in perfluorinated ionomer membranes: structure, properties and applications," J. Membrane Science 120(1996), 1–33.

[75] A. J. Bard and L. R. Faulkner, Electrochemical Methods: Fundamental and Applications, 2nd ed., John Wiley & Sons, Inc., New York, 2000.

[76] R. S. Nicholson and I. Shain, "Theory of stationary electrode polarography. single scan and cyclic methods applied to reversible, irreversible, and kinetic systems," Anal. Chem. 36(1964), 706-723.

[77] G. G. Kim, J. A. Kang, S-J Kim, S. H. Shin and S. J. Kim, "Surface modification of glass epoxy resin using the photocatalytic reaction in TiO2 dispersed solution," J. Alloys & Compounds 449(2008), 184-187.

[78] I. Ruff and V. J. Friedrich, "Transfer diffusion. I. Theoretical," J. Phy. Chem. 75(1971), 3297-3302.

[79] G. J. Janz, G. R. Lakshminarayanan, M. P. Klotzkin and G. E. Mayer, "Diffusion of silver nitrate in concentrated aqueous solutions," J. Phys. Chem. 70(1966), 536-539.